Polymer Blend Compatibilization by Copolymers and Functional Polymers

Jose A. Covas, Luiz Antonio Pessan,
Ana V. Machado, and Nelson M.
Larocca

Introduction

1

Polymer Blends and the Need for Compatibilization

Blending polymers has become an essential and efficient procedure to develop new higher performance polymeric materials having a valuable combination of properties, under relatively short times and with low development and production costs [1-6]. In fact, polymer blending can create materials with targeted properties and competitive prices, allows for fine tuning of the properties via adjustments of composition, and provides an interesting route for plastics waste recycling. The market for polymer blend based materials has increased continuously and significantly during recent decades, especially for automotive, electrical and electronic, packaging, building and construction, and household applications. Polymer blending is usually performed in standard polymer processing equipment, such as twinscrew extruders. Thus, not only the financial risks inherent to the development of new materials are limited, but well-known scale-up, automation, and control techniques are readily available.

Since polymer blends result from the physical combination of at least two polymers, they are usually classified as either miscible or immiscible. As for other mixtures, polymer/polymer miscibility is governed by the laws of thermodynamics [3, 4]. To guarantee thermodynamic miscibility, the free energy of mixing (ΔG_m) should be negative. Since the monomer units in the polymer chains are covalently bonded to each other, the number of ways that they can be arranged in a mixture is limited. Thus, the entropy of mixing (ΔS_m) is very small for polymer mixtures and approaches zero for very high molecular weight polymers. Consequently, thermodynamics predicts that polymer/polymer miscibility has to result from the exothermic heat of mixing ($\Delta H_m < 0$). The latter occurs when the interactions between
neighboring segments of structurally different polymers are energetically more favorable than the intermolecular interactions between segment pairs. Examples of interactions yielding exothermic heats of mixing include hydrogen bonds and dipole-dipole and anionic interactions. However, most of the interesting polymer pairs are immiscible and actually possess poor physical and mechanical properties thus compatibilization is necessary.

2

Compatibilization Routes

The central challenge of the compatibilization of immiscible polymer blends is to generate materials having a stable optimum morphology, that is, to maximize performance under service conditions [7-11]. Interface characteristics such thickness, strength, and interfacial tension strongly determine the bulk properties; poor chemical or physical interaction between two polymers usually implies a high interfacial energy and a low interfacial thickness. Compatibilization is a process of modifying the interfacial properties of immiscible polymer blends, resulting in the reduction of the interfacial tension and in the formation and stabilization of the desired morphology. Thus, compatibilization converts polymer blends into alloys that have the desired set of performance characteristics. In practice, it entails the incorporation of "interfacial agents," "emulsifiers," "adhesion promoters," or, more frequently, "compatibilizers." Usually, the chains of a compatibilizer have a blocky structure, with one constitutive block being miscible with one blend component and a second block being miscible with the other blend component. As a result, a fine and stabilized morphology can be created; the interfacial thickness increases and the interface is strengthened due to the interpenetration of the two types of chains across the interface.

Blend compatibilization can be promoted via several routes [5-11], including (i) ex situ, that is, adding a pre-synthesized copolymer to the components, (ii) in situ, that is, creating a copolymer during blend preparation, (iii) stabilizing the dispersed phase via dynamic vulcanization, or crosslinking, (iv) introducing specific interactions, (v) incorporating ionomers, and (vi) adding a small quantity of a co-solvent - a third component, miscible with both phases. Owing to the large amount of research work and practical applications of each of these routes, this chapter will focus on the compatibilization ex situ, by the addition of a pre-synthesized copolymer and in situ, by creating a copolymer during blend preparation. Machado et al. [11] have compared the efficiency of these two strategies for the compatibilization of polyamide/polyolefin blends. As shown in Figure 7.1, ex situ compatibilization yields the blend with the largest particle size and particle size distribution. Even though both blends exhibit dramatic changes in morphology from $L/D=8$ to $L/D=9$ (screw length/diameter ratio, L/D), morphology development of the in situ blend along the extruder is particularly fast, changes being only perceived up to $L/D=9$. For the other compatibilization route, the initial developments in the first kneading block are also similarly quick, but a regular evolution along the barrel seems to be noticeable.

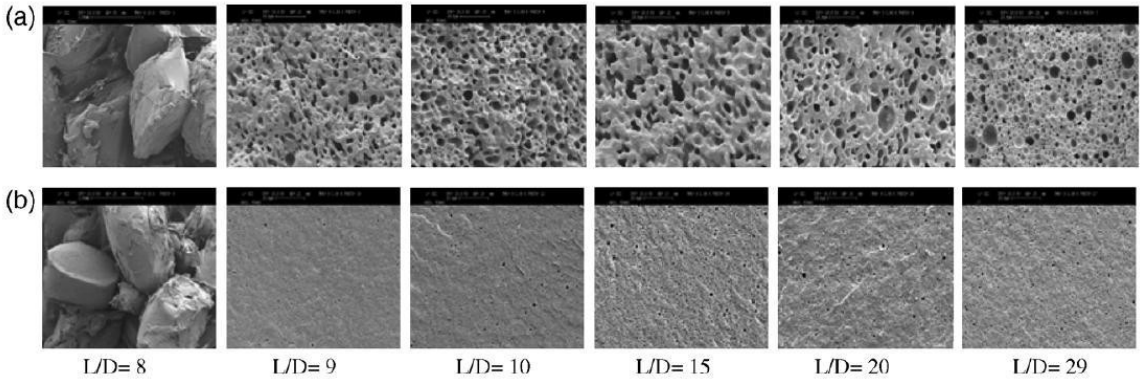

Figure 7.1 Scanning electron microscopy (SEM) micrographs of a polyamide/polyolefin compatibilized blend along the extruder: (a) ex situ and (b) in situ [11].

3 Reactive Extrusion/Processing

The use of extruders as continuous chemical reactors is nowadays commonly known as reactive extrusion (REX) and has proven to be a key technology in the polymer industry [12-14]. As explained above, the growing demands of specialty grades of plastic materials induced an increasing scientific and industrial interest in melt blending and also in the chemical modification of polymers. REX combines two operations traditionally separated, that is, chemical reactions (e.g., for the synthesis or modification of macromolecules, or the in situ compatibilization of polymer blends) and melt processing. Twin-screw extruders are often used, as they comply with the main requirements of REX. Xanthos [12] identified six types of reactions that can be performed by REX: bulk polymerization, grafting, interchain copolymer formation, coupling/crosslinking, controlled degradation, and functionalization (functional group modification).

Currently, REX is an important post-reactor technology to functionalize nonpolar polymers, or to adjust the functionality of polar polymers to specific applications and properties. In the field of polymer blends, functionalized polymers are currently employed to improve the compatibility and adhesion between immiscible polymers by a process called reactive blending.

2 Compatibilization by Copolymers

Ex situ compatibilization, or compatibilization by the addition of a pre-synthesized copolymer, provides an opportunity to easily control the molecular architecture of the additive to be used. Theoretically, block copolymers should seek the interfaces during melt mixing, to decrease unfavorable interactions [15, 16]. Therefore, block or graft copolymers whose segments are chemically identical to, or have affinity with, the polymer components are often used as emulsifiers to reduce the interfacial tension, promote the dispersion of one phase into the other, and stabilize the resulting blend [17]. Hence, the polymeric

compatibilizer to be added to a blend
should have: (i) maximum miscibility with the individual polymeric components, (ii) the molecular weight of each block slightly higher than the molecular entanglement, and (iii) a concentration just above the critical micelle concentration [1].

Initially, the addition of a third polymeric component to a polymer blend was the most common compatibilization method. It was assumed that the compatibilizer would migrate to the interface, broadening the segmental concentration profile. However, it remains to be demonstrated that most of the copolymer added actually proceeds to the interface. Also, there is evidence that the addition of a block or graft copolymer reduces the interfacial tension and alters the molecular structure at the interface, but rarely increases the interphase thickness. Moreover, the actual preparation of the copolymer requires specific chemical routes and reaction conditions.
The influence of a block copolymer on the droplet breakup and coalescence in model immiscible PEP/PPO polymer blends was investigated by Ramic et al. [18], who found that the addition of $0.1\,wt\,\%$ or $1.0\,wt\,\%$ of PEO-b-PPO-b-PEO [poly (ethylene oxide)-poly(propylene oxide) copolymer] triblock copolymers facilitated breakup and inhibited coalescence. The steady-state droplet size resulting from breakup was reduced only slightly by the addition of $0.1\,wt\,\%$ copolymer, but more substantially by addition of $1\,wt\,\%$. However, the kinetics of coalescence were suppressed effectively even when $0.1\,wt\,\%$ of copolymer was added. In these systems, the copolymer seems to reduce the efficiency of both droplet collision and film drainage and/or rupture.

Several researchers [19-24] carried out extensive studies on the use of emulsification curves to evaluate the efficiency of copolymers as compatibilizers. The evolution of the dispersed phase size with copolymer concentration was monitored. After an initial important decrease in the size of the dispersed phase domains with the addition of the copolymer, a leveling-off at higher copolymer concentrations was observed. The shape of the emulsification curve depended both on molecular weight and copolymer molecular architecture and on processing conditions. Similar work was performed by Zhang et al. [25], who studied the compatibilization efficiency of graft copolymers and the effect of the feeding mode on the compatibilization efficiency of polystyrene (PS) and polyamide 6 (PA-6) blends, using the emulsification curve approach. The feeding mode had a major effect on the size of the dispersed phase domains at short mixing times, its effect decreasing, or becoming negligible, at long mixing times. The molecular structure of the polystyrene-polyamide-6 graft copolymer (PS-g-PA-6) also had a profound effect on its compatibilization efficiency. The longer the PA-6 grafts (from 1.7 to $5.1\ \ kg\ \ mol^{-1}$) the higher the compatibilization efficiency. When the PA- 6 grafts were short $\left(1.6-1.7\ \ kg\ \ mol^{-1}\right)$, their number had little effect on compatibility. As for the feeding mode, various studies showed that it can play an important role, but this appears to be blend specific [26-31].

Creton et al. [32] used a series of block copolymers with different molecular weights to compatibilize blends of PS and poly(2-vinylpyridine) (PVP). Only those copolymers whose PVP block polymerization degree was above 200 were found to be effective in preventing failure at the interface. This critical value corresponded roughly to the molecular weight between entanglements (M_e), suggesting therefore
that at least one average "entanglement" between the PVP block and the PVP homopolymer is necessary to have good stress transfer at the interface.

The effect of the molecular weight of block copolymers on the co-continuous morphology of $50/50(w/w)$ PS/HDPE blends (HDPE, high density polyethylene) was investigated by Gallowaya et al. [33] using symmetric polystyrene-polyethylene block copolymers (PS-b-PE) (PE, polyethylene) with molecular weights varying from 6 to $200\ \ kg\ \ mol^{-1}$. An intermediate molecular weight PS-b-PE ($40\ \ kg\ \ mol^{-1}$) showed remarkable results in reducing the phase size and in stabilizing the blend morphology during annealing. Mixing small amounts of 6,100 , or $200\ \ kg\ \ mol^{-1}$ PS-b-PE in the blend did not significantly reduce the phase size, but did decrease the coarsening rate during annealing. The effect of $6\ \ kg\ \ mol^{-1}$ PS-b-PE as morphology stabilizer was inferior to that of 100 and $200\ \ kg\ \ mol^{-1}$. The authors concluded that the existence of an optimal molecular weight block copolymer is due to a balance between the ability of the block copolymer to reach the interface and its relative stabilization effect at the interface.

A-B-A type block copolymers, consisting of styrene end-blocks and butylene, isoprene, or ethylene/butylene mid-blocks, are thermoplastic elastomers exhibiting physical properties typical for rubbers, but with melt processability similar to that of conventional thermoplastics. Besides their success as impact modifiers for several thermoplastics, these materials have been shown to act as compatibilizers for different polymer blends - especially for those of polystyrene or polyesters with polyolefins - where they bridge the blended polymers through physical or chemical interactions. For this purpose, the versatility of SEBS block copolymers can be significantly improved by grafting functional groups, such as maleic anhydride or epoxy groups, to the mid-block that can react, for example, with the end groups of polyamides or polyesters [34-37]. Among others, Sun et al. [38] investigated the compatibility effect of three different styrene-ethylene/butylene-styrene (SEBS) triblock copolymers on the toughness of blends of poly(ethylene terephthalate) (PET) and polypropylene (PP). The compatibilizers involved an unfunctionalized SEBS and two functionalized grades containing either maleic anhydride (MA) (SEBS-g-MA), or glycidyl methacrylate (GMA) (SEBS-g-GMA) grafted to the mid-block. An effect on morphology and impact strength was noticed on adding only $5\,wt\,\%$ of a SEBS copolymer, but this was much more pronounced when using the functionalized copolymers. High toughness combined with rather high stiffness was achieved with SEBS-g-GMA for the PET-rich composition. The addition of the functionalized SEBS copolymers resulted in a finer dispersion of the minor phase and clearly improved the interfacial adhesion. Anastasiadis et al. [39] studied the

compatibilizing effect of block copolymer addition on the interfacial tension between two immiscible homopolymers as a function of additive concentration for the ternary system polystyrene/1,2-polybutadiene/poly(styrene-block-1,2-butadiene). With the addition of small amounts of copolymer, a sharp decrease in interfacial tension was observed, followed by a plateau as the copolymer concentration was increased above the apparent critical micelle concentration.

The effect of molecular weight of atactic polystyrene-b-poly(ethylene-co-butylene)-*b*-atactic polystyrene triblock copolymers on the morphology, impact strength, and
rheological behavior of syndiotactic polystyrene (sPS)/ethylene-propylene rubber (EPR) blends was investigated by Hong and Jo [40]. They observed that the size of the dispersed EPR phase in sPS/EPR/SEBS blends decreases and the particle size distribution becomes narrower with increasing amounts of SEBS in the blends. It was also discovered that the low molecular weight SEBS was more effective in increasing the impact strength than the high molecular weight SEBS. A possible explanation was that the blocks in the low molecular weight SEBS penetrate into the corresponding phase more easily than those with high molecular weight. A comparative study on the compatibility efficiency of styrene-butadiene-styrene (SBS) versus SEBS copolymer on polypropylene/polystyrene (PP/PS, 90/10) blends was carried out by Macaúbas and Demarquette [41]. The morphological, viscosity and interfacial tension results showed that SEBS was a better compatibilizer than SBS.

Various reports [19–25,32–41] on the effects of the copolymer molecular weight and molecular architecture on its compatibilization efficiency for polymer blends rank in the order: tapered diblock > conventional diblock > triblock and smaller molecular weight > higher molecular weight.

3
In Situ Compatibilization or Reactive Blending

In situ compatibilization is based on a specific chemical reaction between two functional polymeric components during blending, and thus is also known as reactive blending [5, 17]. Scheme 7.1 exemplifies reactions that take place at the interface between reactive functional polymers. Because the chemical reaction takes place within the interphase, the copolymer is produced in situ, where it is necessary, with segments from the two homopolymers. The process needs: (i) sufficient
carboxylic acid

Scheme 7.1 Reactive groups and related copolymer formation.
dispersive and distributive mixing to guarantee the required interface regeneration, (ii) the existence of functional groups suitable to react across the interphase, (iii) a sufficiently high reaction rate to make it possible to produce enough copolymer during the residence time in the processing unit, (iv) copolymer stability, and (v) morphology stability. As the copolymer is formed at

the interface, this method generates particularly thick interphases, which thus have good morphology stability.

1

Kinetics of Melt Coupling Reactions at Interfaces

Fredrickson and Milner [42] and O'Shaughnessy et al. [43-48] developed theoretical approaches to the mechanism of interfacial reactions between reactive polymers. Accordingly, the kinetics of copolymer formation at the interface follows basically two time regimes (see also Figure 7.2):

1. In the early reaction stages, the density of functional chains in the interface can be considered to be the same as that of functional chains in the bulk. If the reactivity of the reactive groups is relatively weak, the reaction is rate-controlled and is predicted to follow a second-order reaction rate with respect to the density of copolymers formed at interface (Σ):

$$\frac{d\Sigma}{dt} = k(t) C_a C_b \qquad (7.1)$$

where k is the reaction rate constant and C_a and C_b are the concentrations of the reactive groups at the interface. This second-order rate leads to a linear time dependence of Σ. If the reactivity of the reactive groups is high, the reaction would change to first-order diffusion-controlled kinetics and the time dependence of Σ would no longer be linear.
2) During the subsequent reaction time, the interfacial coverage of the copolymers formed reactively becomes so high that the diffusion of more reactive chains towards the interface is hindered by the dense copolymer brush. In other words, an energy barrier develops delaying the diffusion of further precursor homopolymers towards the interface. This energy appears from the entropy loss due to the location of the homopolymer chains end at the interface and to the stretching of the copolymer blocks in the brush formed at the interface. As a result, the reaction becomes diffusion-controlled and a time dependence of the form $\Sigma \sim t^{1/2}$ is predicted.

Figure 7.2 illustrates the coupling of reactive end-functionalized chains in an interface of finite thickness. While in the early reaction stages the density of the block copolymers formed at the interface is small and the reaction is rate-controlled, at a later reaction stage the interface becomes crammed with block copolymers; for that reason, the chain are stretched and the length of the copolymer chains segments becomes larger than the unperturbed gyration radius (R_g). Owing to the dense copolymer brush at the interface, the diffusion of further reactive specimens towards that same interface decreases significantly, causing a large reduction of the reaction rate, which becomes diffusion-controlled.

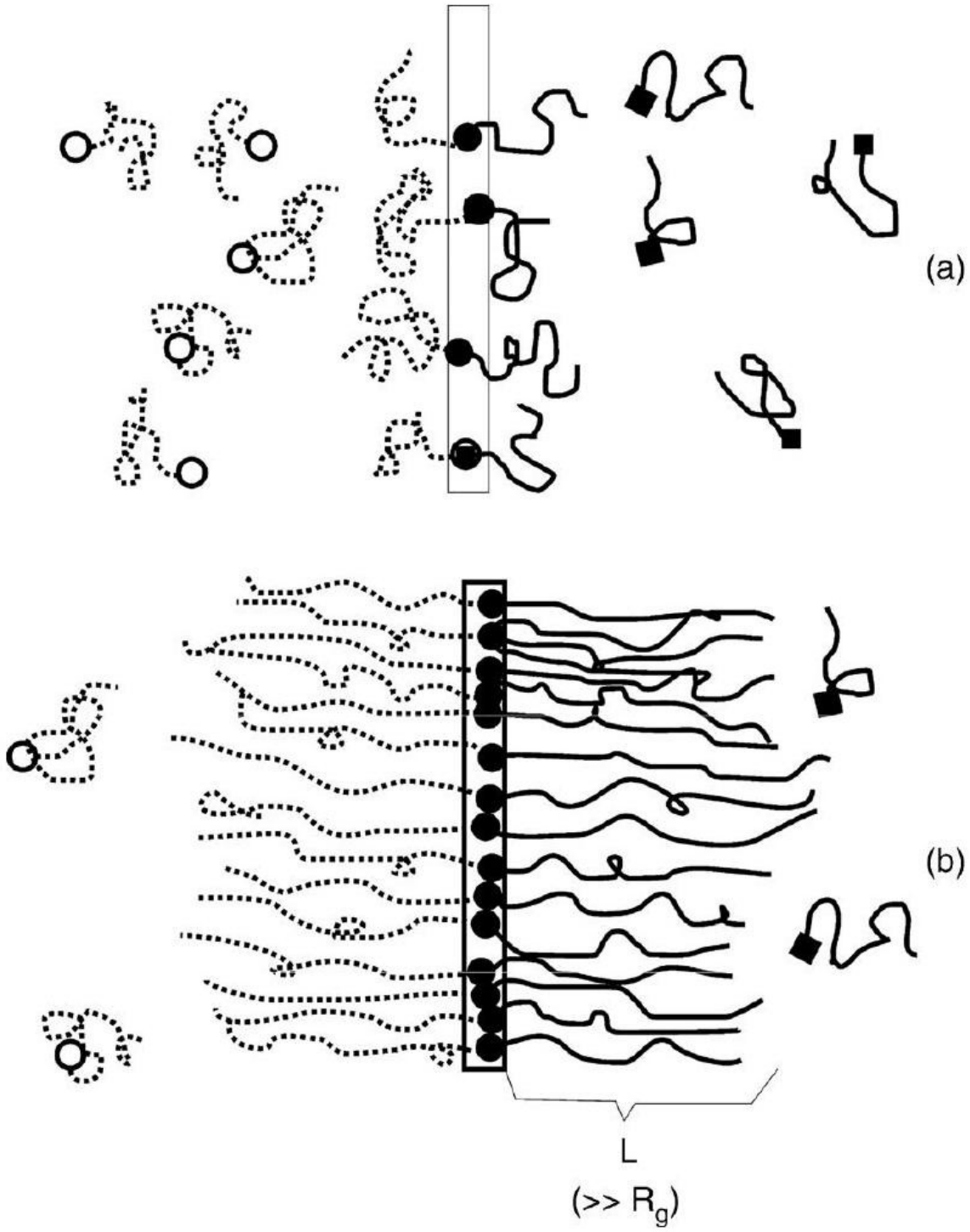

Figure 7.2 Schematic of the coupling of reactive end-functionalized chains in an interface of finite thickness: (a) initially, the density of block copolymers formed at the interface is small and the reaction is ratecontrolled; (b) later, the interface becomes full of block copolymers, hence the chains are stretched and the length of the copolymer chains segments becomes larger than the unperturbed gyration radius (R_g). Adapted from Reference [46].

Several studies confirmed that the coupling reactions in the first time regime are indeed reaction-controlled for the most common reactive pairs, epoxy/carboxylic acid [49, 50] and anhydride/aliphatic amine [51, 52]. For polymers functionalized with these reactive pairs, it was found that chain ends can get to the interface well before the occurrence of reactions [50,51], that is, the characteristic reaction time is larger than the characteristic diffusion time. The magnitude of the reaction activation energy is also an indicator that the reaction kinetics are reaction controlled. For example, Oyama and Inoue [52] estimated a value of $120\ \ kJ\ \ mol^{-1}$ for reactions between the pair amine/anhydride. This high value is characteristic of a chemical process, in contrast with physical diffusion, which is expected to have a low activation energy ($¿30\ \ kJ\ \ mol^{-1}$).

The reaction rate constant, k, is governed mainly by temperature and reactivity of the complementary functional groups in the polymers. The k values of various pairs of the latter were determined by Orr et al. [53]. Again for the epoxy/carboxylic acid and anhydride/aliphatic amine pairs, values around 2.1 and $1400\ \ kg\ \ mol^{-1}\cdot\ \ min^{-1}$, respectively, at $180^{\circ}C$, were reported for precursor chains with a molecular weight of about $25\ \ kg\ \ mol^{-1}$. For the reactive pair amine/epoxy, the authors found a k of about $0.2\ \ kg\ \ mol^{-1}\cdot\ \ min^{-1}$. Noticeably, despite of the large k for the reactive pair amine/ anhydride, the reaction between polymeric precursors containing these reactive groups was shown to be rate controlled at common processing temperatures [50-52, 54]. The reactions with carboxylic acid and amine are particularly important, as several commercial polymers have at chains ends these functional groups; for example, polyesters are end-functionalized with carboxylic acid groups and polyamides are end-functionalized with amine groups. Consequently, the potential reactive precursors for the reactive compatibilization of blends containing polyesters and polyamides are polymers functionalized with epoxy and anhydride groups, respectively.

2
Effect of Interfacial Reactions on the Interface Morphology

Various studies relating to the morphology of static reactive interfaces demonstrated that these can become highly irregular after the reaction between the reactive precursors [55-58]. A few researchers [59-63] measured the interfaces irregularity as a function of the reaction time and compared them with the Σ values determined experimentally. A continuous increase in interface roughness with increasing Σ was observed, but that increase becomes sharp as Σ reaches a critical value. Using selfconsistent mean-field theory, SCMFT, methods (described by Shull [64]), the interfacial tension was calculated from Σ values. It was found that this sharp increase takes place when Σ reaches the value corresponding to the absence of the interfacial tension [59]. Molecular dynamics simulations also predict the emergence of irregularities when the interfacial tension fades away [65]. Since the interfacial tension is given by $\gamma = dE/dA$, where dE is the variation of free energy and dA is the variation of the interfacial area, if γ vanishes there is no longer a free-energy penalty associated with the

creation of a new interfacial area. Consequently, large curvatures may arise at the interface, due to thermal fluctuations. As more reactive chains migrate to the freshly created interfacial area, more interfacial copolymer is formed and this area is progressively covered. In turn, this gradual covering keeps the interfacial tension small; the interface curvature can further develop, eventually creating a very rough interface, a process known as interface roughening.

If the roughness grows to a sufficiently great extent, large droplet-like protuberances of one phase are formed. These are known as pinch-offs and can eventually become completely encapsulated by the interface crowded with copolymers. In this case, micro-emulsions can form inside one of the phases. These micro-emulsions have a dimension around 100 nm and consist of a homopolymer surrounded by the interfacial copolymers. Figure 7.3 illustrates the formation of a pinch-off in an interface and the consequent formation of micro-emulsions. Evidence of the formation of pinch-offs and micro-emulsions was observed by Kim et al. [57] in the interface of PS-end-carboxylic/PMMA-ran-epoxy (PMMA, poly(methyl methacrylate)), as the interfacial reaction progressed for more than 6 h at $180^{\circ}C$. In this work, it was noted that the pinch-offs grow only towards the PMMA phase, and that the micro-emulsions are likewise formed in this phase. This takes place because the micro-emulsions are more stable if their graft chains have the branched portions situated outside the micro-emulsion curvature, as in this case the steric hindrance of the branched chains is minimized. In addition to the micro-emulsions, smaller particles (most probably micelles) are also formed. Micelles contain only copolymers and their size is approximately equal to the radius of gyration of the copolymer (about 20 nm). Evidences of interfacial pinch-offs were also observed by Zhang et al. [60] and Lyu et al. [58] for reactive static interfaces of PS-end- NH_2/¿ PMMA-end-anhydride after 1 h of reaction. However, in these experiments insufficient time was given to the eventual development of micro-emulsions and micelles.

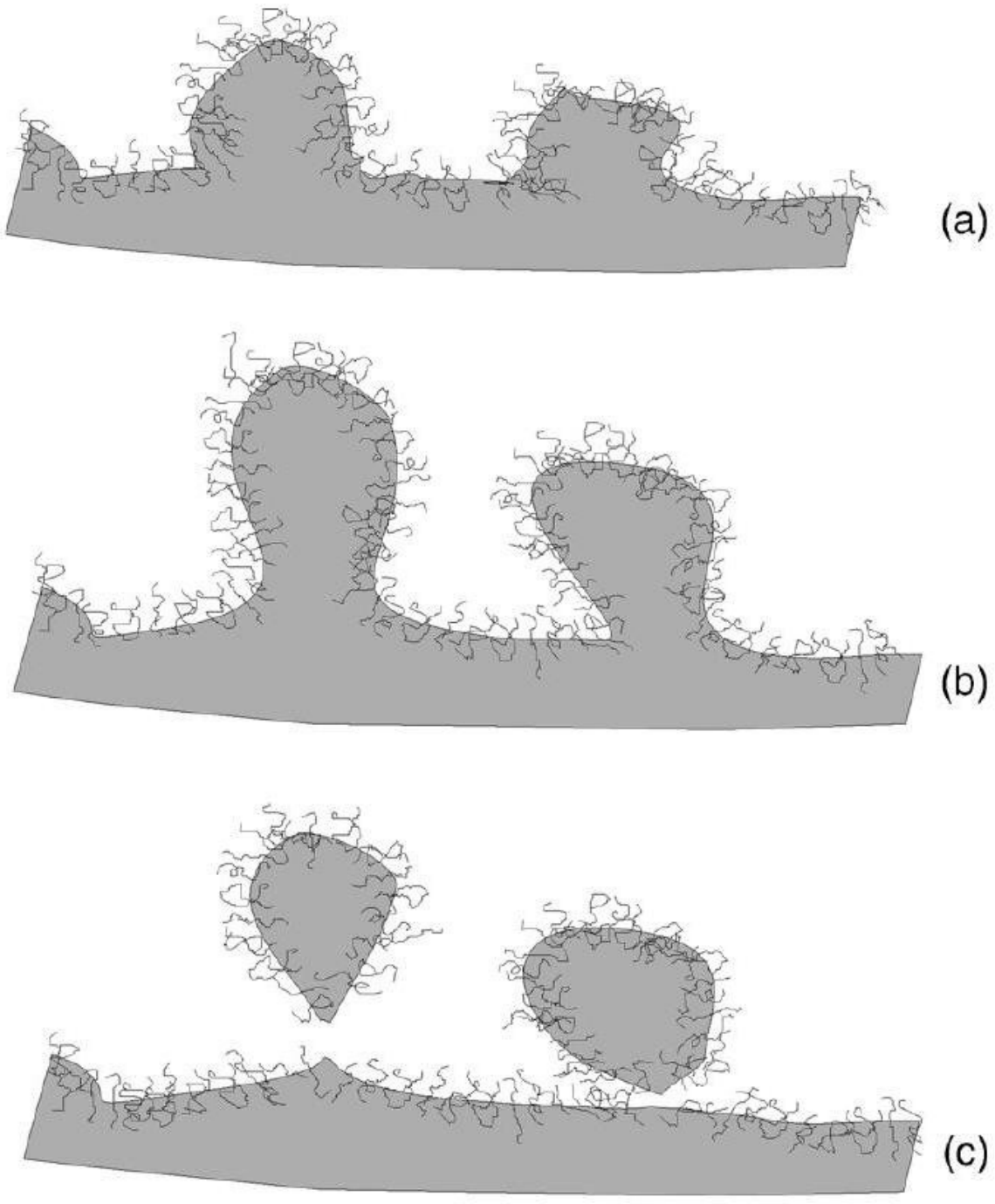

Figure 7.3 Evolution of the interfacial morphology due to crowding of the interface by interfacial copolymers and consequent decrease of the interfacial tension: (a) interfacial roughening; (b) formation of pinch-offs; and (c) formation of micro-emulsions on the continuous phase.

3 Effect of the Interfacial Copolymer Structure

Jeon et al. [66] investigated the effect of the interfacial copolymer precursor structure on the reaction rate constant (k). The authors used PMMA chains end-functionalized and mid-functionalized with phthalic anhydride. Both were reacted with PS chains
end-functionalized with amine groups, that is, block and graft copolymers were formed at the interface. Under static (no-flow) conditions, the k value for the reactions of the end-functionalized chains is more than ten times higher than that for midfunctionalized chains, that is, it is faster to form block than graft copolymers at reactive interfaces. This was attributed to a higher segregation of chain ends to the interface as compared with the bulk, due to polymer dynamics [67]. Under flow conditions, the k ratio between end- and mid-functionalized chains decreases from 10 to 2.6-3.2. Probably, the shear flow induced convection reduces the concentration of the chains ends at the interface in comparison with the concentration of the chains ends at equilibrium. The effect of flow will be discussed later in more detail. The higher reaction rate constant for end-functionalized chains, as compared with the mid-functionalized ones, was confirmed by Jeon et al. [68], who studied 70/30 PA-6,6/ PS blends (PA6,6 = polyamide 6,6) containing as reactive precursors PS chains endfunctionalized with anhydride groups and random functionalized with the same groups, that is, SMA (styrene-maleic anhydride) copolymers. By comparing blends with the same concentration of functionalized PS, it was observed that those containing end-functionalized PS chains presented faster conversion.

Another important feature concerning the formation of graft copolymers on the interface is the grafting efficiency. Jeon et al. [66] reported that even though the SMA has on average 6.4 anhydride groups per chain, only nearly two PA-6,6 chains were grafted per SMA chain. This is due to the effect of the steric hindrance in the SMA chains already grafted by a PA-6,6 chain, in addition to the restricted interfacial volume at the interface. As described above, the interfacial reaction can only occur in the interface, which is a few nanometers thick. Since it is unlikely that the SMA copolymer extends fully along the interface, there are actually few anhydride groups per SMA chain available for the reaction. This low grafting efficiency at interfaces of polymer chains with random reactive groups has also been reported for reactive blends of PS-carboxylic/PMMA-epoxy [59, 69] and PBT/PS-epoxy (PBT, poly(butylene terephthalate)) [70].

4 Effect of the Reactive Precursor Molecular Weight

Several studies demonstrated that the reaction rate at the interface depends on the reactive precursor molecular weight (functional polymer), being higher for lower molecular weights [55, 71, 72]. This effect cannot be associated with the diffusion of the low molecular weight chains, since several studies evidenced that the interfacial reaction is controlled by the collision efficiency of the reactive groups and not by diffusion. Instead, Yin et al. [55] proposed that the dependence

of the reactivity on the molecular weight could be related to the interfacial thickness, as shown by Helfand and Tagami [73] and Broseta et al. [74]. As described before, the reaction rate at the interface usually decreases dramatically as the critical concentration of interfacial copolymers is formed. Thus, the reaction at the interface can be suppressed before the interfacial tension vanishes and, therefore, extensive roughening may not occur. Owing to this effect of rate decrease, the interfacial roughness is likely to be larger for low molecular weight reactive precursors, since low molecular weight reactive chains are more able to diffuse through the copolymer barrier, to reach the interface and to continue the reactions. Furthermore, self-consistent mean field theory [73, 74] predicts that the critical value of Σ that minimizes the interfacial tension decreases with the molecular weight of the interfacial copolymer. In fact, it has been shown that the roughening at the interface is larger for low molecular weight reactive chains [55].

5 Effect of the Flow

In industry, reactive polymer blends are generally prepared in conventional compounding machines, such as continuous extruders, or batch-type internal mixers, which promote complex melt flow patterns. The flow can influence significantly the reaction kinetics. Several studies have shown that the reactive blends prepared under flow have reaction rate constants more than 1000 times higher than those of reactive blends prepared in static bilayer films [56, 72, 75]. This effect of flow on the reaction rate is not yet well understood, but Jeon et al. [66] speculated that it can be due to convection, which can increase the collision probability between the reactive groups of the polymers at interface. These authors also conjectured that the increase of the reaction rate due to flow can be overestimated, as the initial stages of morphology development of immiscible polymer blends in mixers is very complex and therefore the interfacial area at this stage could be much larger than that found in the final stage of the completely developed blend.

Flow also induces the formation of micro-emulsions, as it can detach the pinch-offs from the interface. As shown by Kim et al. [76] for a bilayer of reactive PS-endcarboxylic and PMMA-ran-epoxy, micro-emulsions could be observed in a shear flow under a shear rate of $100\ s^{-1}$ after less than 50 min , while for static conditions they would form after 15 h [57]. In the case of melt blends prepared in internal mixers, micro-emulsions could be detected after less than 5 min of mixing, thus demonstrating again the importance of flow [68].

Apart from pinch-offs detachment, flow may also speed up the pull-out of copolymers from the interface and their subsequent dispersion as micelles in the continuous blend phase. This pull-out mechanism depends on the frictional shear force exerted on the interfacial copolymer chains, which is determined by the thermodynamical interaction of the interfacial copolymer chain with the blend chains at each phase and by the molecular weight and structure of the copolymer chains [77]. The experimental studies of Inoue et al. [77-79] corroborate the

frictional theory and show that the pull-out tendency depends on the structure of the interfacial copolymer, on its molecular weight, and on the intensity of shear stress during flow:

1. It is easier to pull-out a linear block copolymer formed at the interface than a graft copolymer with a branch structure located at the dispersed phase. However, graft copolymers whose branch structure is located at the continuous phase (where the external shear forces are acting) have a higher tendency to be pulled out. The number of grafted chains of the continuous phase attached to the backbone continuous phase becomes higher and, therefore, there will be a considerable tendency for the migration of the graft chains to the continuous phase, forming micelles. These can be avoided by increasing the molecular weight of the reactive precursor copolymer and/or reducing the copolymer functionality [68]. Figure 7.4 illustrates the effect of the interfacial copolymer structure.
2. The pull-out tendency also depends on the molecular weight of the copolymers. This tendency increases as the molecular weight of the copolymer segment miscible in the continuous blend phase increases and the molecular weight of the segment miscible in the dispersed phase decreases. It is very likely that pullout occurs for a copolymer having a segment miscible in the dispersed phase with a molecular weight close or below its critical entanglement molecular weight (M_c). For example, if the segment miscible in the dispersed phase is PMMA, then pull-out is expected if the molecular weight of this segment is below $10000\ \ g\ \ mol^{-1}$, which is the M_c of PMMA [80].
3. Since the frictional shear force increases with shear stress, pull-out is more likely to occur at high shear rates $(\dot{\gamma})$ and high matrix viscosity, $\eta(\tau = \dot{\gamma}\eta)$.

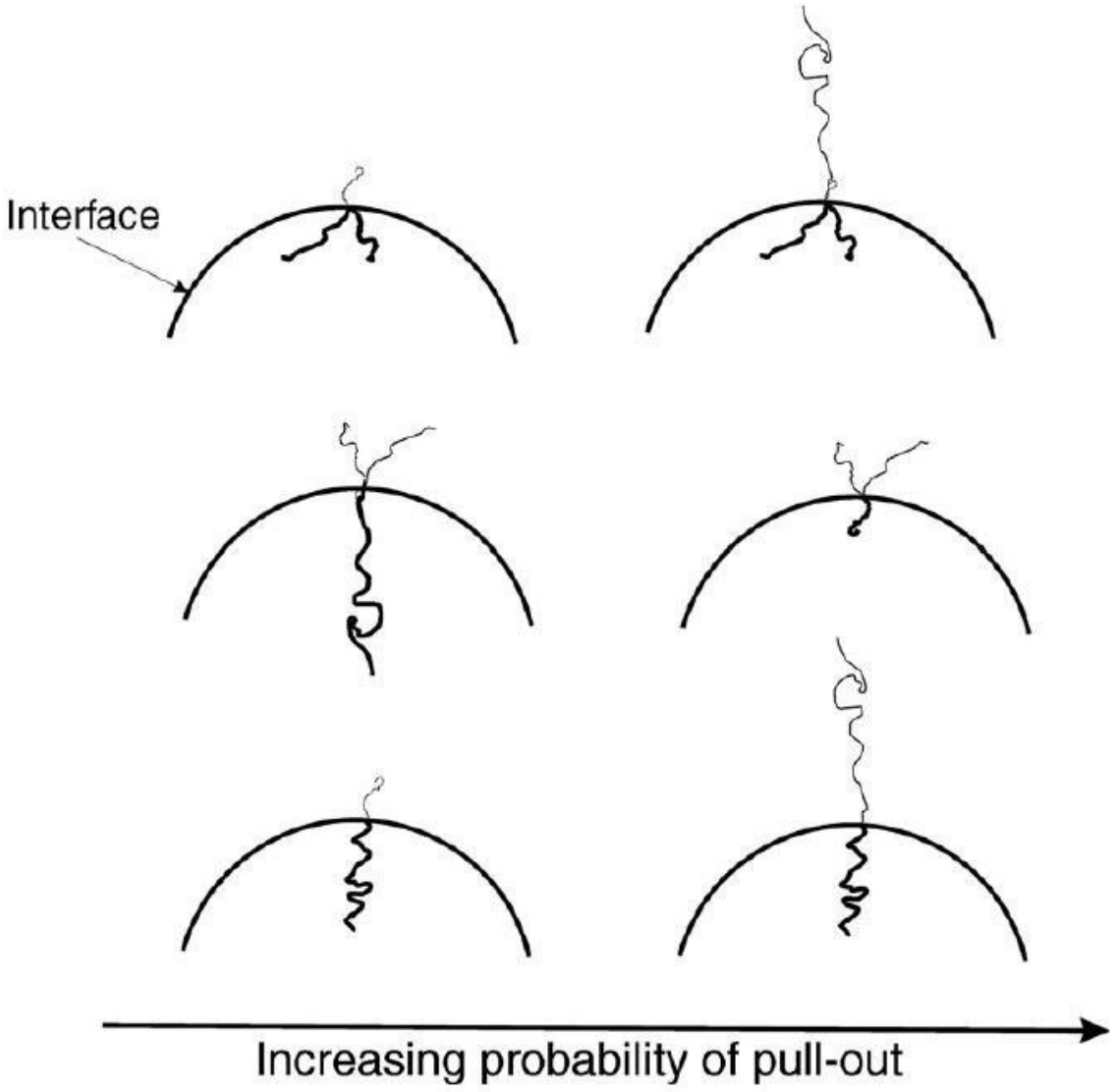

Figure 7.4 Pull-out tendency of block and graft copolymers at the interface, for varying molecular weight of the segments. Adapted from Reference [77].
of the reactive copolymer should also be considered. If there are many chains grafted, the thermodynamic interaction of the graft copolymer with the

Inoue et al. [77-79] showed that micelles can be formed at the matrix even when the interfacial copolymer is a symmetric block copolymer. This is not predicted by the theory of block copolymers at interfaces [81], which asserts that only very asymmetric block copolymers are unstable and tend to depart from the interface, forming micelles in the phase where the longer block of the copolymer is miscible. In fact, this theory does not account for the effect of the shear stress, which has an important role on the stability of the interfacial copolymers at interfaces, as seen above.

The formation of micro-emulsions and/or micelles in blends with reactive interfacial copolymers should be avoided, because if the copolymers leave the

interface (by interfacial roughening or by pull-out), the interfacial coverage of the dispersed phase decreases and, therefore, its interfacial tension and coalescence increases, leading to a blend with a coarser morphology. This effect was clearly demonstrated by Jeon et al. [68] for PA-6,6/PS blends with PA-6,6 as the continuous phase. The authors used end-functionalized PS with anhydride groups with two molecular weights ($10000\ \ g\ \ mol^{-1}$ (PS10) and $37000\ \ g\ \ mol^{-1}$ (PS40)) as reactive interfacial precursors. Blends containing $2\,wt\,\%$ of reactive precursors PS10 presented tiny 50 nm particles dispersed in the PA-6,6 phase, which could not be detected in the blends with PS40. These particles are micro-emulsions of block copolymers that were removed from the interface by interfacial roughening and/or a pull-out mechanism. As discussed above, interfacial roughening and pull-out mechanisms are both more likely to occur for low molecular weight reactive precursors, such as PS10. As the copolymers in the micro-emulsion/micelles are removed from the PS/PA-6,6 interface, the interfacial coverage of copolymers in the surface of PS particles becomes lower in the blend with PS10 than in the blend with PS40 and as a result the average PS particle size is larger in the former than in the latter.

6 Role of the Reaction Rate on the Dispersed Phase Morphology

Morphology control is an important constraint to create polymer blends with enhanced properties [5]. During blending, the size of the dispersed phase changes from millimeters to micro and/or nano dimensions. Morphology development is influenced by the composition, the viscosity of the components and their viscosity ratio, and the processing conditions (operating conditions, type of geometry of the mixing equipment) [82].

There has been much speculation regarding the mechanisms of particle size reduction and the effect of the interfacial reaction on morphology development. Karger-Kocsis and Vergnes [83] reported no significant changes in morphology between 5 and 40 min of mixing PP/rubber blends. Favis and Chalifoux [84] prepared PP/PC blends (PC, polycarbonate) in a batch mixer and concluded that the most significant changes in morphology occurred during the first 2 min of mixing, when melting and softening of the materials would also occur. Scott and Macosko [85, 86] showed that at short mixing times the two phases are sheared into ribbon or sheet structures, which will subsequently breakup due to shear and interfacial tension. Sundararaj et al. [87-89] provided evidence that the most significant morphology development of a PS/PP blend in a twin-screw extruder occurred in the first two disks of the first kneading section. They also detected sheet structures and demonstrated that, after the initial breakup, the particle size was not reduced significantly. Moreover, they observed a phase inversion mechanism when the minor component melted or softened at a lower temperature than the major component. Cartier and Hu [90] studied the preparation of PP/PA-6 blends in a twin-screw extruder and concluded that the morphology develops very rapidly, but even faster in the case of in situ compatibilized blends with PP grafted with maleic anhydride (PP-g-MA). In this case, the size of the dispersed phase undergoes an abrupt reduction

from a few millimeters to sub-micrometer levels during the transition from solid pellets to a viscoelastic fluid, with the final morphology being attained as soon as that transition is completed. In systems containing rubber and polyamide/polyesters, the rubber phase is dispersed from millimeter to micrometer level within a few seconds [91]. This means a decrease of the diffusion distance of the polycondensate chains to the rubber interface by a factor of 10^3 and an increase of the interface by a factor of 10^9, that is, the rate of interfacial reactions is dramatically enhanced. In the case of PA-6/ EPM-g-MA blends (EPM-g-MA, ethylene and propylene monomer grafted with maleic anhydride) the reaction is so fast that as interfaces are created upon melting they become immediately covered with PA-6 chains, causing a quick reduction of the interfacial tension and preventing coalescence, which induces a further refinement of the dispersed phase.

To study the morphology progression of PA-6/EPM-g-MA blends, Machado et al. [92, 93] developed a technique to rapidly collect samples from fully filled sections of a twin-screw extruder. It was shown that at the beginning of the melting zone, even though the material was mostly solid, the non-reacted MA content decreased to less than half of its original value. One screw turn later, a fully melted conventional polymer blend morphology was present, with relatively good distributive and dispersive mixing levels, having caused a further important reduction in MA (Figure 7.5). Before the end of the extruder, a stable and controlled morphology had been achieved.

The stability of PA-6/EPM-g-MA compatibilized blends was evaluated by measuring the average particle size of the dispersed phase after processing by injection molding and capillary rheometry. No changes could be detected, that is, the blend morphology was stable [11].

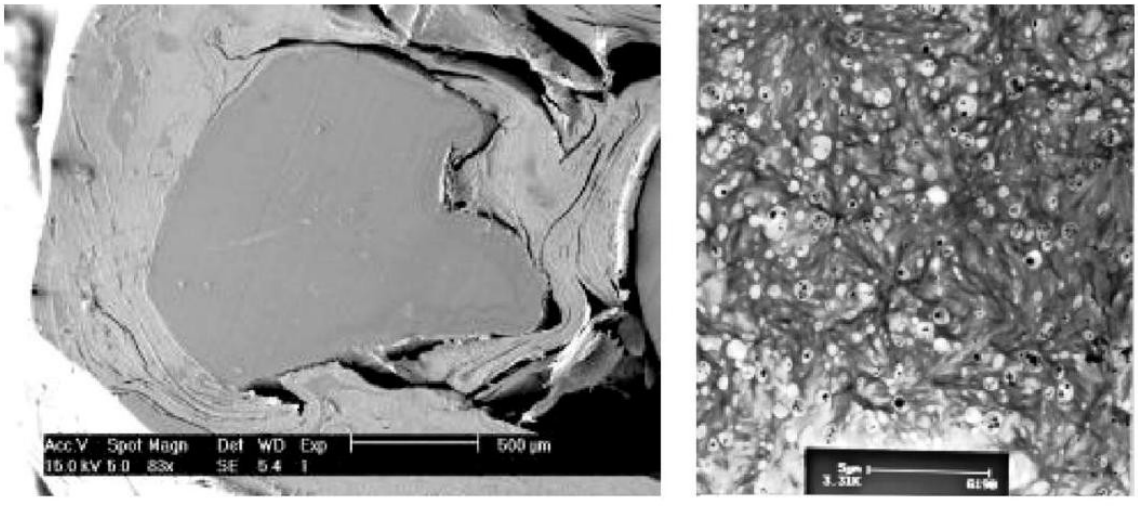

L/D = 12 L/D = 13

Figure 7.5 Morphological evolution along the extruder (L/D, screw length to diameter ratio) of a PA-6/EPM-g-MA blend.

When a blend is prepared by melt mixing under high shear rates, the interfacial area increases due to the progressive break-up of the dispersed phase caused by the shear stress. When these particles run into each other coalescence may occur, which increases their size [94-96]. Various studies have suggested that the main function of interfacial copolymers is actually to suppress this coalescence, thus yielding a reduction in the size of the dispersed phase, and that this suppression takes place if the interfacial area coverage reaches a minimum value, Σ_{min} , [88, 94-98]. It has been shown that Σ_{min} is lower than the maximum interface coverage, Σ_o, and that its value depends on the thermodynamic interactions between the polymers. For instance, for the PS/PMMA system, Σ_o is 0.171 or 0.131 chains nm^{-2} for interfacial copolymers with a molecular weight of 38000 or 84000 $g\ mol^{-1}$, respectively [72], but the Σ_{min} value that suppresses dynamic coalescence is about 0.02 chains nm^{-2}. This means that only about 20 % interfacial coverage is necessary to stabilize the morphology. Conversely, for the PS/PE system, Σ_o is 0.25 chains nm^{-2} for a molecular weight of 40000 $g\ mol^{-1}$, while Σ_{min} is around 0.2 chains nm^{-2}, that is, in this case it is necessary to cover 80 % of the interface to suppress coalescence [98].

Owing to the dynamics of the breakup/coalescence process, the formation of interfacial copolymers should be fast enough to promote at least an interfacial coverage of Σ_{min} in any interface created by break-up before coalescence develops, otherwise the average particle size increases. To achieve a very fine dispersed phase, it is necessary to ensure a very high reaction rate, since the interfacial area is large and, for that reason, a high concentration of interfacial copolymers should be formed. As a result, there is a correlation between the size of the dispersed phase and the reaction rate, which means that the desired blend morphology can be achieved by adjusting the parameters that influence the reaction rate, such as the concentration of reactive groups, the molecular weight of the reactive chains, the type of reactive groups, and so on.

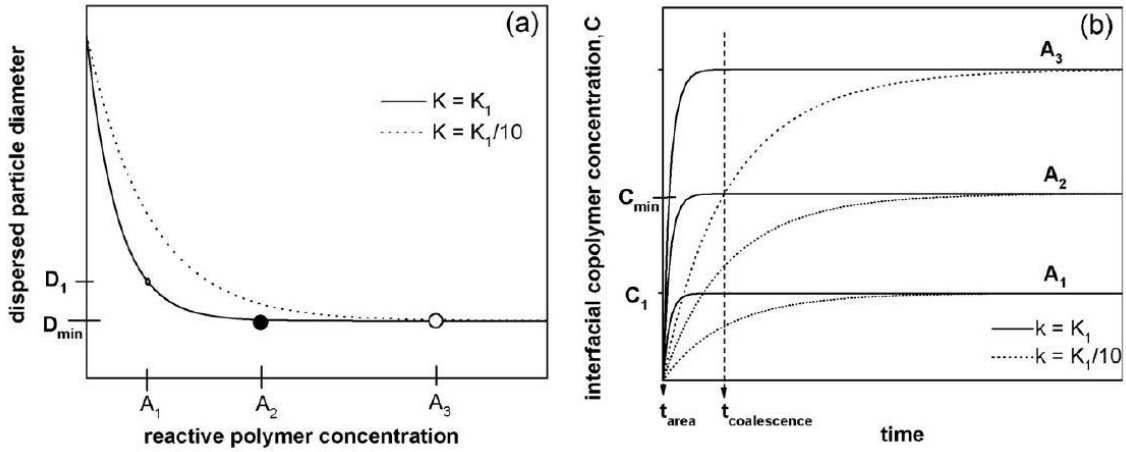

Figure 7.6 Average size of the dispersed phase as a function of the concentration of reactive groups (a); concentration of interfacial copolymer (b).

Figure 7.6a illustrates how the average size of the dispersed phase of a reactive blend changes with the growing concentration, C, of reactive groups. Clearly, the particle size decreases exponentially and levels off at a given concentration. This behavior has been described extensively in the literature [49, 99, 100] and can be explained by the change with time of the concentration of copolymer formed at the interface. To simulate the kinetics of this reaction, it is assumed that the concentration, A, of the reactive groups at the interface is low, which means that the reactions at the interface end before the formation of a densely packed brush of copolymers. The resulting equation follows second-order reaction kinetics and the concentration of interfacial copolymer follows a correlation of the type $C \propto -\exp(-t)$.

Figure 7.6b shows this second-order kinetics for various concentrations of A reactive groups (or concentrations of the polymer containing these groups). This figure also identifies the concentration of interfacial copolymer $C_{\min}$ that should be formed at the interface to completely suppress coalescence, that is, the coverage $\Sigma_{\min}$ in a blend with a dispersed phase particle size of D_{min}. The stabilization of this morphology can only take place if $C_{\min}$ is attained at the interface before coalescence begins, that is, before time $t_{\text{coalescence}}$; this occurs when the concentration of A is A_2, as seen in Figure 7.6b. If A is below A_2 (say A_1), the concentration of copolymer formed between t_{area} and $t_{\text{coalescence}}$ is C_1, which is lower than $C_{\text{min.}}$. As the copolymer concentration is now insufficient to form a Σ_{min} coverage on the particles with D_{min}, coalescence takes place and D will increase (decreasing the interfacial area) up to D_1, when the coverage reaches $\Sigma_{\min}$ for concentration C_1. Conversely, if $A > A_2$ (e.g., A_3), the copolymer concentration formed between t_{area} and $t_{\text{coalescence}}$ is C_3, higher than $C_{\min}$. Now, the copolymer concentration induces a coverage larger than $\Sigma_{\min}$ on the particles with D_{min}, but this does not promote a further reduction in particle size below $D_{\min}$, because the minimum size of the dispersed particles is governed only by the breakup process, which is hardly affected by the interfacial coverage. Therefore, for a concentration $A > A_2$, a leveling off is observed in Figure 7.6a.

Figure 7.6b also demonstrates the effect of decreasing the reaction rate (by reducing the reaction rate constant, k) on the relation between particle diameter and the concentration A of reactive group. At constant A, decreasing k from k_1 to $k_1/¿$ 10 (dashed lines) slows down the rate of copolymer formation, causing a reduction of the concentration of copolymer at the interface until the initiation of coalescence, $t_{\text{coalescence}}$. Therefore, at concentration A_2, the amount of copolymer formed until $t_{\text{coalescence}}$ is lower than C_{min} and, as a result, coalescence occurs. For the slower reaction, the formation of $C_{\min}$ before the beginning of coalescence only occurs when A increases from A_2 to A_3. As a consequence, the beginning of the plateau is also shifted from A_2 to A_3, meaning that a slower reaction requires more reactive polymer to suppress coalescence. Notably, in addition to k, the

other parameters discussed above that influence the rate of copolymer formation can promote similar results in terms of morphology.

In summary, the concentration of interfacial copolymers that suppresses coalescence is increased by:

- Enhancing the reaction rate constant, k. This can be accomplished increasing the temperature and/or altering the reactive groups pairs, for instance, changing the pair carboxylic/epoxy for amine/anhydride.
- Reducing the molecular weight of the reactive polymer. However, the molecular weight should not be too small, to avoid the formation of micro-emulsions and micelles, as discussed above.
- Utilizing polymers with end-functionalized reactive groups, instead of polymers with reactive groups distributed along the chains. This means the formation of block copolymers at the interfaces instead of grafted ones.
- Boosting the thermodynamic interactions between the two phases and, consequently, the interfacial width.

7

Examples of Applications of Reactive Blending in Polyester and Polyamide Blends

This section presents and discusses a few examples of reactive blending during the preparation of polyester and polyamide blends, by reaction of epoxy/carboxylic acid (polyesters blends) and anhydride/amine (polyamide blends) groups.

Polybutadiene Terephthalate Blends

PBT/ABS blends boast a potentially attractive combination of good mechanical properties and processability: while PBTprovides stiffness and good melt processability, the rubber from ABS offers impact resistance and the SAN (styrene-acrylonitrilecopolymer) from ABS (acrylonitrile-butadiene-styrene copolymer) confers increased Heat Deflection Temperature (HDT) [99]. However, these blends have a relatively high brittle-ductile transition temperature, BDTT , limiting their use at low temperatures. The high BDTT is normally attributed to the existence of coarse ABS particles dispersed in the PBT matrix. Some authors have suggested that BDTT depends not only on particle size but also on interparticle distance, with a coarse morphology causing a larger interparticle distance [100-107]. Furthermore, there is evidence that the morphology of melt compounded PBT/ABS blends is unstable when they are injection molded [99].

The incorporation of reactive species in these blends can decrease the size of the ABS particles and thus reduce the BDTT. An efficient reactive precursor is the copolymer MGE (methyl methacrylate-glycidyl methacrylate-ethyl acrylate copolymer), which is a copolymer of methyl methacrylate (MMA)-glycidyl

methacrylate (GMA)-ethyl acrylate (EA). The MGE copolymer is miscible with the SAN phase of ABS [108], its synthesis is relatively simple [108], and only small quantities (about 5 wt %) are necessary for blend compatibilization. Since SAN is the continuous phase in ABS, in a PBT/ABS blend most of the MGE dissolved in SAN is in contact with the PBT phase. Owing to this SAN/PBT interface, during melt processing the epoxy groups of glycidyl methacrylate will react with the carboxylic groups of the PBTchains that are located at this interface, forming a graft copolymer of PBT-g-MGE. PBT chains can also have hydroxyl groups at the chains ends that may also react with the epoxy groups of MGE. However, the reaction epoxy-hydroxyl is less probable to occur than the epoxy-carboxyl one, since it has been shown that the reaction rate of the former is slower than that of the latter [109, 110]. Figure 7.7 shows the effect of the incorporation of MGE on the phase-dispersed morphology of a PBT/ABS blend. The effect of MGE on the morphology and other properties of PBT/ABS blends has been studied extensively [111-114].

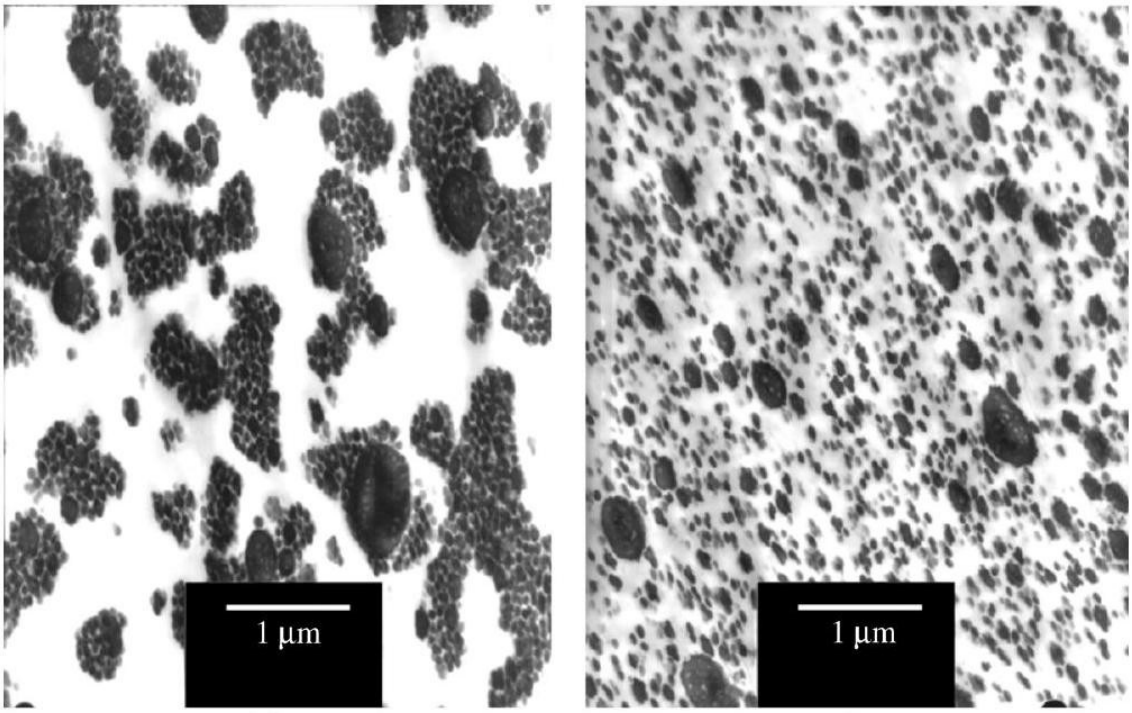

Figure 7.7 Dispersion of ABS particles in PBT/ABS blends containing $30\,wt\,\%ABS$: (a) without compatibilizer MGE and (b) with 5 wt% MGE (Ambrósio, J.D., Lanea, N.M., Pessan, L.A., and Hage, E.: unpublished results).

MGE was used by Mantovani et al. [115] in PBT/ABS blends containing $40\,wt\,\%$ ABS. The BDTT was -10 and $-50^{\circ}C$ for the blends without and with compatibilizer ($5\,wt\,\%$), respectively. This drop was associated with the better dispersion of the ABS particles obtained with the incorporation of MGE.

However, a decrease of the impact strength at room temperature relative to the physical blend was reported. Hale et al. [111], who obtained similar results, speculated that this decrease is due to the crosslinking that takes place in addition to the reactions that form the graft copolymers at the interface. The occurrence of crosslinking reactions between PBT and polymers functionalized with epoxy groups has also been described by Martin et al. [116]. Crosslinking reactions can occur due to the bifunctionality of PBT. Since its chains can have carboxylic groups at both chain ends, the PBT molecules can act as a crosslinking agent between the chains containing epoxy groups. It is also possible that the chains with epoxy groups act as crosslinks. This can occur if the epoxy group opens and creates alcohol functionalities, which can react with other epoxy groups present in other chains. Hale et al. [111] have also found evidence that acid residues of polymerization found in ABS can act as catalysts of these reactions.

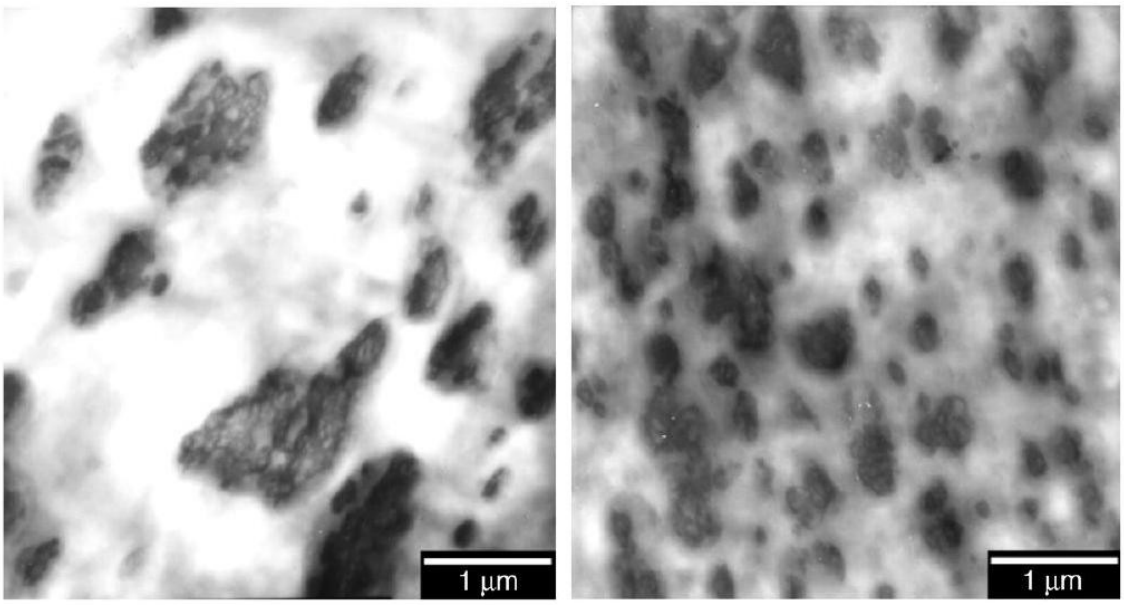

Figure 7.8 Effect of MGE on the dispersed phase morphology of a PBT/AES blend containing 30 *wt* % AES without compatibilizer (a) and with 5 *wt* % of MGE (MGE contains 10 *wt* % GMA) compatibilizer (b) (Larocca, N.M., Hage, E., and Pessan, L.A.: unpublished results).

MGE copolymers are also efficient reactive precursors to compatibilize PBT/AES blends. Since AES (acrylonitrile-ethylene-styrene copolymer) is itself a two-phase blend, consisting of EPDM grafted to SAN, it is likely that MGE can promote coalescence suppression in PBT/AES through a mechanism similar to that found in PBT/ABS/MGE blends. In fact, Figure 7.8 shows that the incorporation of MGE leadsto a better dispersion of AES particles in PBT/AES blends. PBT/AES

blends containing $30\,wt\,\%$ of AES, with and without MGE copolymers, were studied by Larocca et al. [117, 118]. Evidence that in situ reactions took place upon MGE incorporation includes the large increase in blend viscosity and the refinement of the blend morphology. As the epoxy concentration in the blend increases, the AES particles size reduces. This decrease levels off when the concentration of GMA in the blend reaches $0.5\,wt\,\%$. The decrease in particle size of AES seems to be correlated with the DBTT of the blends, as it decreases exponentially up to the GMA concentration of $0.5\,wt\,\%$ and then also levels off. In the case of a PBT/SAN model blend containing $5\,wt\,\%$ of MGE, the dependence of the SAN particles size on the GMA concentration in MGE also follows an exponential decrease and the particle diameter also levels off for the GMA concentration of $0.5\,wt\,\%$. The analogous performance of both DBTT and dispersed particle size clearly indicates that MGE reduces the DBTT through reduction of the dispersed phase particle size.

Larocca et al. [118] also studied the influence of the molecular weight of MGE containing $10\,wt\,\%$ GMA on the morphology and DBTT of PBT/AES/MGE blends. As the molecular weight of MGE decreases from 380000 to $120000\ \ g\ \ mol^{-1}$, the DBTT decreases from -5 to $-17^{\circ}C$ and the morphology becomes finer. However, a further decrease in molecular weight leads to higher DBTTs. As discussed previously, low molecular weight reactive polymers promote a faster reaction rate and the formation of more copolymer at the interface, thus hindering coalescence more efficiently and, consequently, causing a decrease in AES particles size and a concomitant decrease in DBTT. However, in the case of a too low MGE molecular weight, pull-out of the low molecular weight interfacial copolymer and/or interfacial roughening could occur [55, 77-79], generating a decrease of the copolymer interfacial coverage and a consequent increase of the coalescence of AES particles.

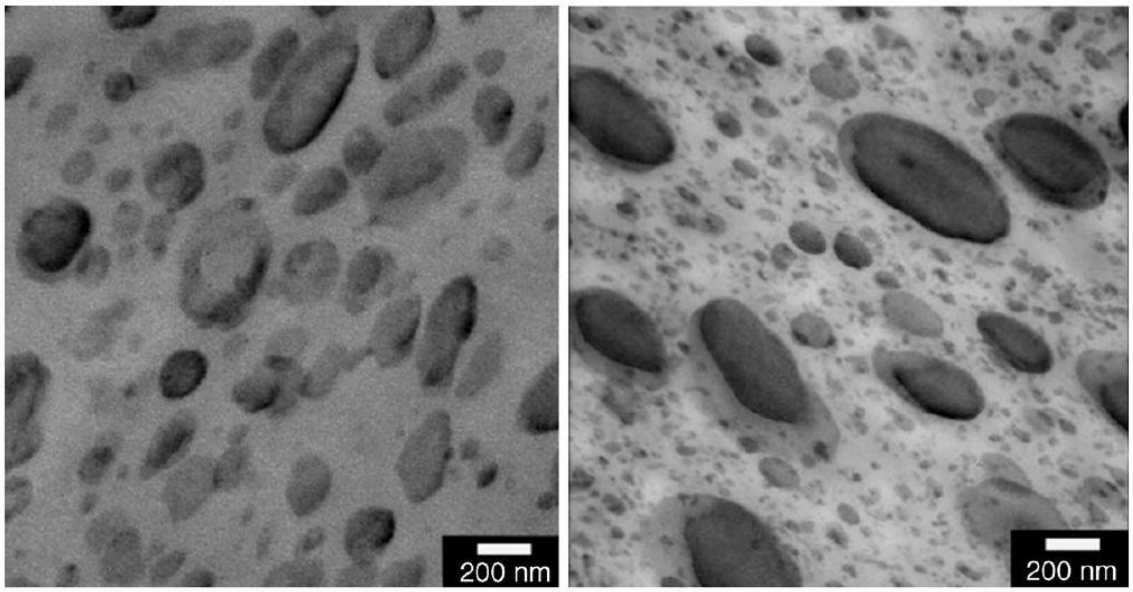

Figure 7.9 Effect of MGE molecular weight on the morphology of PBT/SAN blends containing $20\,wt\,\%$ SAN with high molecular weight MGE (a) and low molecular weight MGE (b) (Larocca, N.M., Hage, E., and Pessan, L.A.: unpublished results).

In fact, it has been observed that low molecular weight MGE copolymers really lead to the formation of micelles and/or micro-emulsions in the PBT/SAN/MGE blend (Figure 7.9). Figure 7.9b shows the presence of tiny micro-emulsions, in addition to the presence of larger SAN particles. Both blends contain $5\,wt\,\%$ of MGE, which, in turn, contains $10\,wt\,\%$ of GMA. PBT/SAN/MGE is a suitable model blend for the study of interfacial reactions in the more complex PBT/ABS/MGE blend, since in both cases the interfacial reactions take place in the PBT/SAN interface.

Another reactive copolymer containing epoxy groups, with possible commercial attractiveness, is polystyrene-glycidyl methacrylate (PS-GMA). Its synthesis is also simple and it can compatibilize blends of PBT with polymers containing styrene moieties, such as SBS. PS-GMA is miscible with polystyrene, at least when it has low molecular weight and low GMA concentration [119]. Studied PBT/SBS/PS-GMA blends where some SBS and PS-GMA characteristics were varied. They observed that most blends did not show signs of a decrease of DBTT with increasing PS-GMA content; neither was there a morphology refinement of the SBS dispersed phase. This was explained by the microphase separation of the SBS copolymer at the processing temperatures (about $240^{\circ}C$). As the microphase develops, the SBS morphology becomes lamellar, with alternating lamellas of PS and PB. This reduces the interfacial PBT/PS area, deterring the formation of the interfacial copolymers that would stabilize the SBS particles against coalescence. Nevertheless, a DBTT decrease was observed when a SBS with high polystyrene content ($38\,wt\,\%$) and long polystyrene blocks (about $20000\ \ g\ \ mol^{-1}$) and a PS-

GMA with moderate GMA content ($4\,wt\,\%$) and high molecular weight (about $35000\ \ g\ \ mol^{-1}$) were used. These characteristics favored a higher PBT/PS interface, as well as the miscibility of the PS-GMA and PS phases, enabling graft copolymer formation at the interface.

Polyamide-6 Blends

Polyamide-6 is a widely used engineering thermoplastic also suitable to be used in reactive blends due to the amine and carboxylic functional groups present in its chains ends. Likewise, compatibilized PBT/ABS and compatibilized PA-6/ABS blends have attracted great interest, due to their very attractive combination of properties [120-123]. Araújo et al. [124-128] studied the effect of two compatibilizers, MGE and copolymers of methyl methacrylate-maleic anhydride (MMA-MA), on the morphology and properties of PA-6/ABS blends. These copolymers were selected because the epoxy groups of MGE can react with the carboxyl and amine groups of polyamide, whereas the maleic anhydride (MA) groups of MMA-MA can react only with the amine groups of polyamide. Moreover, MGE and MMA-MA are miscible with the SAN phase of ABS, hence it is expected that interfacial reactions take place at the interface of PA-6/SAN, forming grafted copolymers of PA-6-g-MGE or PA-6-g-MMA-MA. While PA-6/ABS blends containing $50\,wt\,\%$ ABS possess a notched Izod impact strength around $70\ \ J\ \ m^{-1}$ (until $90^{\circ}C$), the incorporation of only $5\,wt\,\%$ of MMA-MA containing $3\,wt\,\%$ of maleic anhydride created a super-tough blend, with an impact strength on the order of $800\ \ J\ \ m^{-1}$, holding until a temperature of $-10^{\circ}C$. However, when using MGE instead of MMA-MA, no super-tough blends at any temperature were generated, even when adding $5\,wt\,\%$ of MGE containing $10\,wt\,\%$ of GMA. The significant improvement in impact strength of the PA-6/ABS blends containing MMA-MA can be accounted by the morphological changes caused by the incorporation of this compatibilizer. PA-6/ABS blends have a coarse dispersion of ABS in the PA matrix that causes their low impact strength. However, blends containing $5\,wt\,\%$ of MMA-MA show a refinement of the ABS dispersion. This decrease of particle size is due to the formation of graft copolymers at the PA-6/SAN interface. The larger coalescence suppression efficiency of the reactive compatibilizer containing anhydride groups, as compared with the reactive compatibilizer containing epoxy groups, is coherent with the very high reaction rate of the pair cyclic anhydride/amine versus the slower reaction rate of the pairs epoxy/amine and epoxy/ carboxylic acid [53].

To better understand the interfacial reactions of the PA-6/ABS/MMA-MA system, studies using the simpler amorphous PA/SAN/MMA-MA model blend were conducted by Becker et al. [129-131]. For blends containing $5\,wt\,\%$ of MMA-MA, these authors found a minimum in the SAN particle size at $1\,wt\,\%$ of MA in the compatibilizer. At higher MA content in the MMA-MA, an increase of the SAN particles size was observed. It was speculated that the graft copolymers formed from the MMA-MA compatibilizer with higher MA content are more easily pulled-out from the polyamide/SAN amorphous interface, which would significantly diminish the interfacial coverage of the SAN particles and make

them more susceptible to coalescence. This conjecture is corroborated by the increased blends viscosity, as well as by the presence of micelles of graft copolymers on the matrix of these blends.

The reactive compatibilization of PA-6/polyolefins blends using polyolefins containing MA was studied by Machado et al. [11, 92, 132, 133]. It was shown that the MA content of the modified polyolefins decreases strongly upon melting of the PA pellets and melt flow through the first set of staggering kneading blocks, that is, the grafting reaction is very fast. Simultaneously, the morphology changed dramatically in this zone of the extruder, from mm to (sub) μm level. It was also observed that the final morphology depends on the amount of the copolymer formed at the interface and on the processing conditions used.

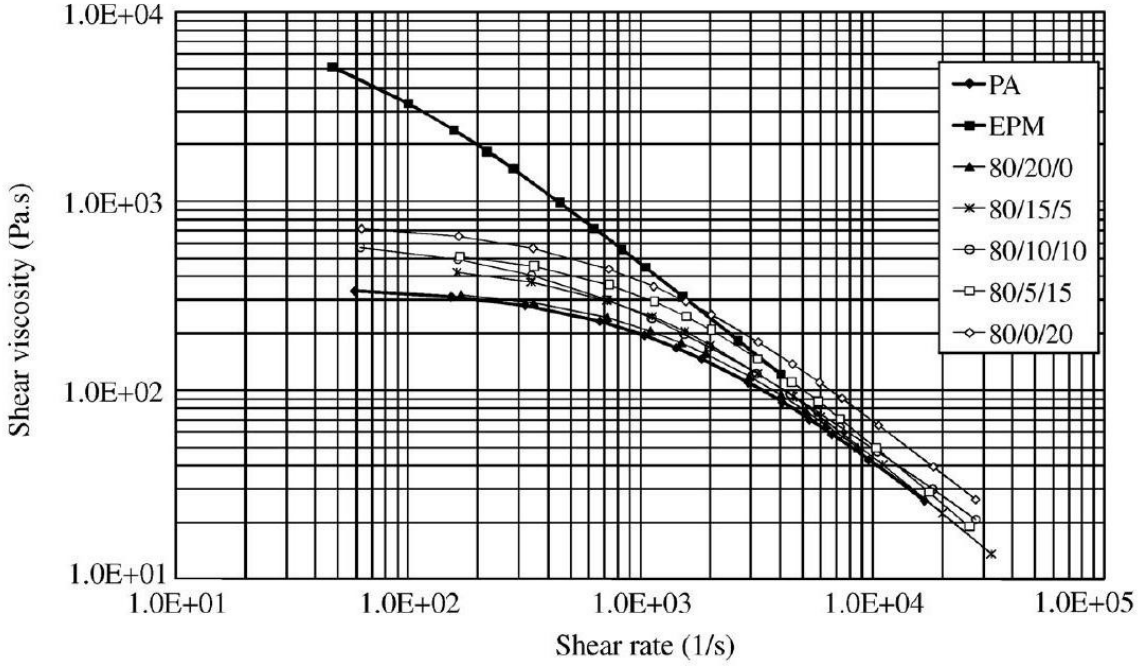

Figure 7.10 Shear flow curves of the original polymers (PA and EPM) and of their extruded blends. Adapted from Reference [134].

The rheological behavior of PA-6/EPM/EPM-g-MA (80/20/0 to 80/0/20 $w/w/w$) blends was also investigated [134]. The flow curves depicted in Figure 7.10 show that at high shear rates the viscosity of all materials, except the compatibilized blend (80/0/20), is very similar. For the non-compatible PA-6/EPM blend the viscosity curve is similar to that of the PA-6 reference. The increase in viscosity with increasing EPM-g-MA content was attributed to an increase of the interfacial adhesion as a result of in situ compatibilizer formation. Moreover, the viscosity of the blends increases with increasing MA content in the rubber phase, that is, with the amount of copolymer formed at the interface. The shape of the curves indicates that the rheology of the blends is mainly governed by the matrix,

but the shift between the curves also suggests that other parameters also play a role.

4
Application to Manufacturing of Polymer Blends

1
Equipment

Introduction

Successful reactive extrusion, that is, the combination of melt extrusion and chemical reactions in a single operation to continuously polymerize monomers and/or modify
polymers, requires not only that the reactions to take place inside the extruder be compatible with the general characteristics of these machines, but also that the extruders selected have certain constructional and functional features. Despite its obvious advantages and practical success, especially in the last 15-20 years, reactive extrusion is a complex technology, which requires simultaneously mastering plasticating extrusion and controlling a chemical reaction under very specific conditions. For the purposes of reactive extrusion, chemical reactions should [12, 14, 135-138]:

- have low activation energy and be rapid; for example, in the case of polymer blending, the polymers should have either a high concentration of reactive groups or these should be highly reactive, to ensure a high conversion into copolymers;
- involve reagents that are stable at the usual compounding temperatures;
- yield reaction sub-products that can be easily removed;
- not be affected by the instabilities that are inherent to the extrusion process.

Modern reactive extrusion operations can be multifaceted and involve a series of individual steps, such as feeding the components (either together or sequentially), melting them (but liquid ingredients may also be utilized), melt mixing the composition (distributive and dispersive homogenization), devolatilizing, and die forming for subsequent pelletization. Therefore, an extruder is adequate to be used as a chemical reactor if it:

- guarantees efficient control and adjustment of output, temperature, and residence time;
- creates a thermally homogeneous environment, provides efficient interfacial generation, and good mixing;

- is able to work with materials that may present a wide range of characteristics (gas, solid, powder, fluids (namely with high viscosity levels);
- allows the sequential addition of the reaction ingredients (monomer, polymer, water, solvent, reactant, etc.);
- provides the efficient removal of sub-products or of low molecular weight by-products via devolatilization;
- allows working in an inert atmosphere;
- can be easily attached to downstream pelletization equipment.

Single-screw extruders began to be used as chemical reactors for polymerization purposes in the 1950s, to ensure continuous production, avoid the use of solvents and bring about energy savings (e.g., through elimination of solvent heating and cooling) [139]. During the following two decades these machines were also applied for polymer chain breaking and grafting of monomers to polyolefins. However, and despite the progressive improvements in pressure generation and distributive mixing efficiency, single-screw extruders offer limited sequential addition capabilities, which confines their application to relatively simple operations, such as modification of polyolefins with peroxide, or silane grafting [140].

Counter-rotating and co-rotating twin-screw extruders, or combinations of various types of equipments [136, 141], have been progressively recognized as more suitable to the specificities of some chemical reactions. Counter-rotating intermeshing self-
wiping twin-screw extruders fulfill most of the requirements listed above, but they can only operate at low screw speeds (typically below 50 rpm , to minimize the pressure developing in the mechanical calender gap, in the screws intermeshing zone, which pushes them against the barrel wall, generating wear). Consequently, shear rate levels are moderate and so is the dispersion efficiency. Copolymerization of styrene- *n*-butyl methacrylate, polymerization of ε-caprolactam, grafting of maleic anhydride onto polyethylene, polymerization of urethanes, and radical polymerization of methacrylates are examples of reactions performed using this machine [142]. Non-intermeshing counter-rotating extruders are utilized for polycondensation reactions, as they provide excellent distributive mixing even at low shear rates, but they have limited pressure generation capacity and dispersive mixing efficiency.

Co-rotating intermeshing twin-screw extruders are currently the most widely used for reactive extrusion. The output of commercial machines can range from a few kilograms to around 100 tonnes per hour. In general, they possess the following features:

- modular construction, whereby the geometries of both the screws and barrel can be adapted to the specific needs of each application, in terms of the feeding sequence of the components, of the melting location, of the

mixing type and intensity (the total deformation resulting from local flow fields and flow time), of the average residence time, or of the devolatilization location and level;

- independent control over output and screw speed, enabling operation in starve fed mode (i.e., the screws work partially filled over a significant portion of their length), which facilitates the introduction or the removal of ingredients and byproducts, respectively, decreases the total mechanical power consumption and helps to control melt temperature (by allowing for thermal relaxation to take place after viscous dissipation during flow in mixing zones);
- the screws can rotate at high screw speeds (up to ¿ $1500\,rpm$), thus promoting high dispersion levels whilst guaranteeing high production rates;
- they generate the pressure required for melt flow through a pelletizing die or, via the insertion of a gear pump between extruder and die, for the direct extrusion of a final product (e.g., reactive spinning of elastomeric polyolefin fibers [143]).

Nevertheless, only a limited number of the chemical reactions performed in batch reactors can be transposed to reactive extrusion, due to the following shortcomings of extruders:

- Residence times in extruders are very short (frequently, less than 1 min); hence very fast kinetics, high conversion, and selectivity are necessary.
- Since extruders have limited cooling capacity, exothermal reactions, or highly viscous media (inducing significant viscous dissipation) must be avoided, as they can induce side reactions (e.g., thermal degradation), the severity of this problem increasing with the size of the extruder, as heat transfer becomes progressively less efficient.
- Owing to the complexity of the thermo-mechanical environment inside of an extruder, and the difficulty in monitoring the evolution of the physicochemical phenomena along the screw axis, it is difficult to scale-up a laboratorial production to industrial application. This explains the current scientific and technological interest in process modeling and optimization.

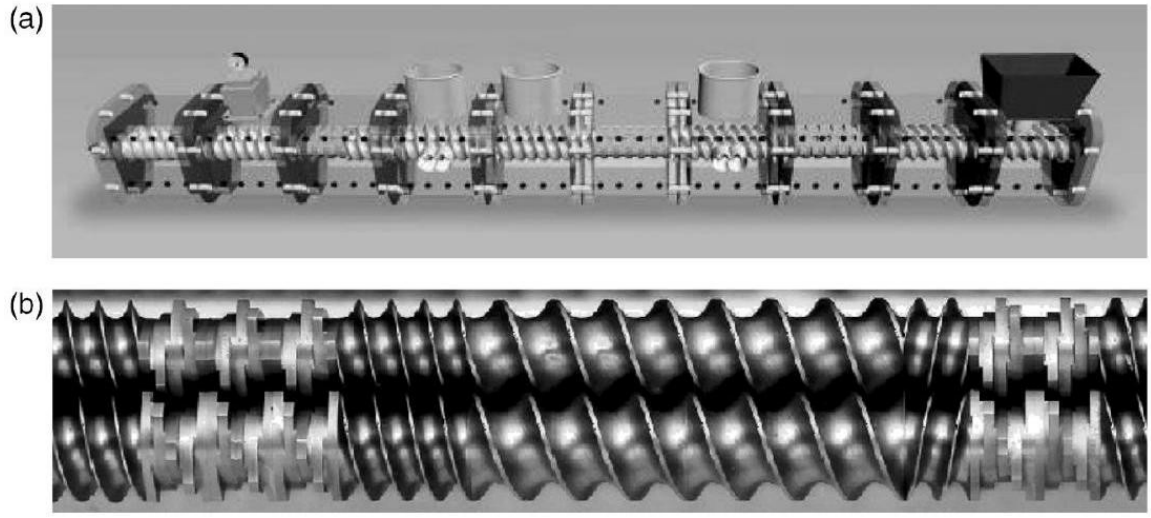

Figure 7.11 Intermeshing co-rotating twin-screw extruder: (a) extruder set-up, with multiple vents, devolatilization, and side feedings [144]; (b) section of a typical screw profile (www.coperion.com).

Main Operational Features of Co-rotating Twin-Screw Extruders

As shown in Figure 7.11, an intermeshing co-rotating twin-screw extruder consists of two parallel screws - interpenetrating mechanically as much as possible - rotating at the same speed inside a hollow heated barrel. Each screw is generally built by assembling a certain number of individual elements along a shaft, while the barrel results from coupling together unit modules in such a way that the assemblage may contain various apertures in the downstream direction for feeding and/or devolatilization purposes. Thus, quite distinct extruders can be created by the proper selection of screw and barrel elements. Figure 7.11 also shows that the screw profile can be quite complex, encompassing conventional conveying sections separated by mixing zones that induce different levels and types of mixing, depending on their geometry and length. Figure 7.12 presents some of the most common types of commercial screw elements. Conveying/screw type elements give rise to conveying sections that drag the material downstream and induce some distributive mixing. A kneading element contains several disks staggered with a positive, neutral, or negative angle (the disk thickness and staggering angle may also vary); one or several adjacent elements of this type create a kneading block in the screw. As the staggering angle changes from positive to neutral and negative, the conveying capacity decreases, becomes nil, or negative, and the levels of distributive and dispersive mixing increase. At the right-end side of Figure 7.11b one may identify a conveying element with a negative helix, which is often used to create an effect similar to that of a negative kneading block. These last two types of elements are generally known as "restrictive," in terms of their flow conveying capacity. Table 7.1 summarizes the conveying and mixing characteristics of the most widespread types of screw elements.

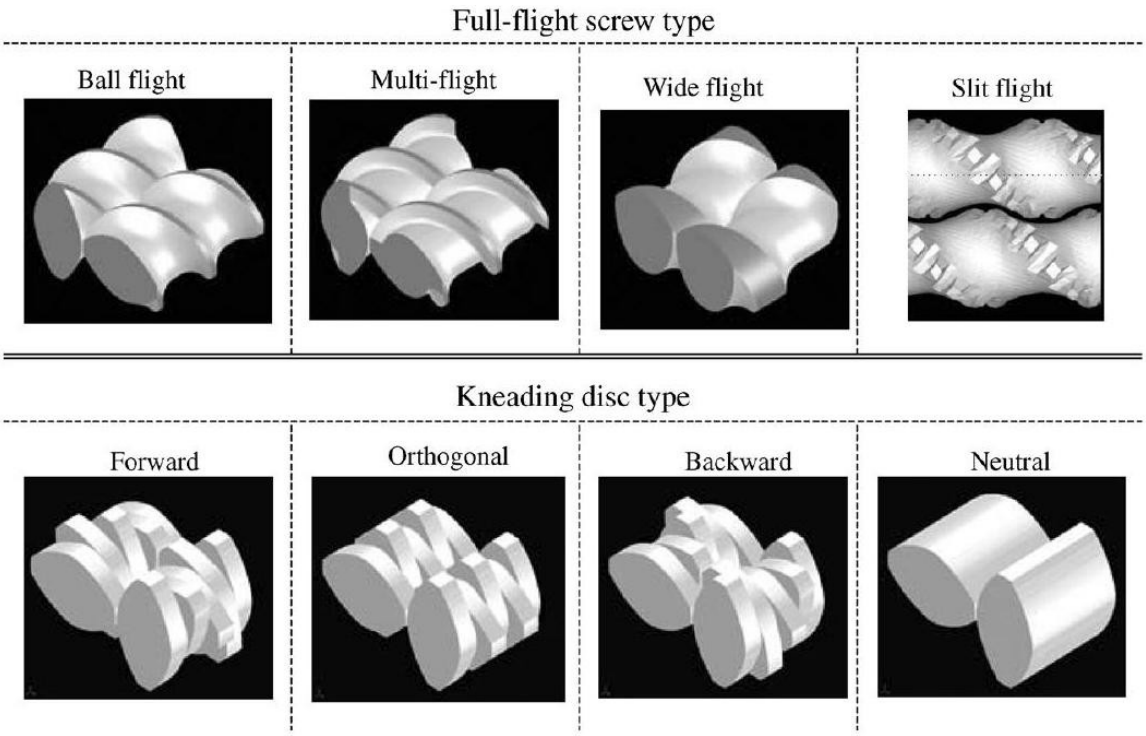

Figure 7.12 Representative individual screw elements used in twin-screw extruders [137].

As noted above, these machines operate in starve fed mode, that is, the output is determined by the feeding rate of volumetric or gravimetric raw material feeders, not by the screw speed. When the material enters the extruder, it follows a figure-ofeight flow pattern along the channels of the partially-filled conveying elements (Figure 7.13). The figure also demonstrates that instead of having a continuous channel from hopper to die, as in the case of the single-screw extruder, here the rotation of the screws originates three independent flow channels (for a double-start screw), whose volume expands and reduces upon rotation, thus inherently bringing on some distributive mixing.

Table 7.1 Main characteristics of conveying elements and kneading blocks of twin-screw extruders [a] ((a) and (b) should not be directly compared) [44].

		Mixing			
		Conveying	Distributive	Dispersive	Local residence time
(a) Conveying	Low	+	+	o	+ + +
elements	Medium	+ +	+	o	+ +

(helix angle)	High	+ + +	+	o	+
	Negative	-	+ + +	+ +	+ + + +
(b) Kneading	Positive (low)	+ +	+	o	+
blocks	Positive	+	+ +	+	+ +
angle)	Orthogonal	o	+ + +	+ + +	+ + +
	Negative	-	+	+ + +	+ + + +

a) + + + + very high; + + + high; + + medium; + low; o nil; - negative.

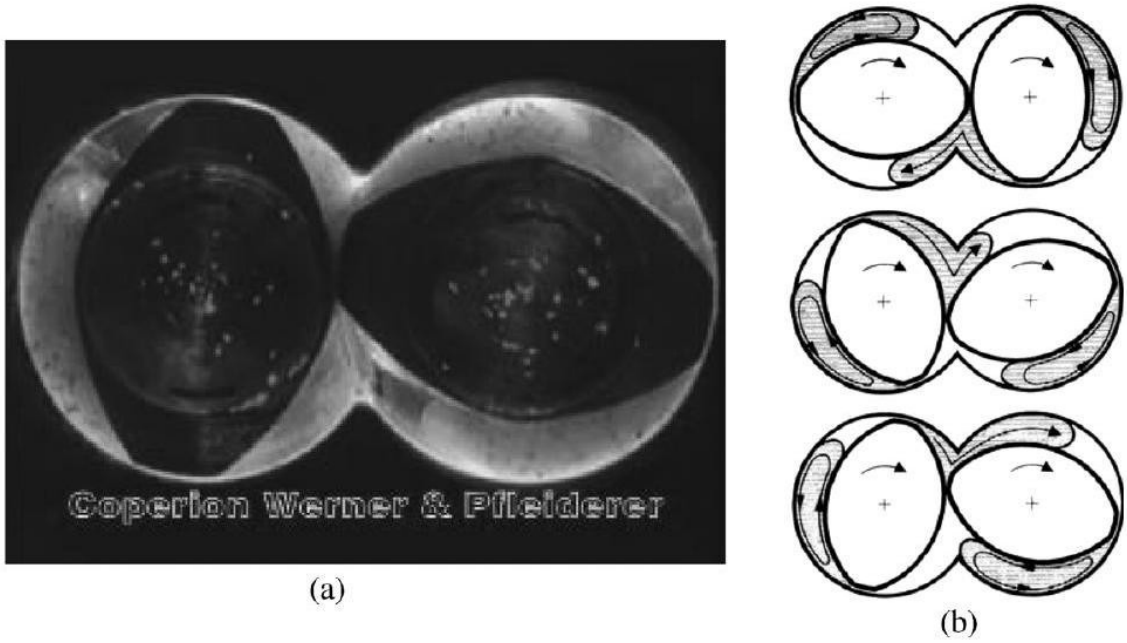

Figure 7.13 (a) Cross-section of a twin-screw extruder; (b) figure-of-eight flow pattern. (a) Courtesy of Coperion Werner & Pfleiderer; (b) adapted from Reference [145].

Once the flow reaches a restrictive zone, it must generate the pressure required to overcome the resistance created by the latter and continue its progression towards the die. Consequently, the material accumulates directly upstream of that restriction, filling up a few screw turns and spending longer local residence times before traversing it. The higher the restriction (defined by its geometry and length), the higher the pressure to be generated, and the higher the number of screw turns upstream working fully filled. Accordingly, restrictive elements

generate locally more efficient heat transfer, create a complex 3D flow (particularly in the apex region) - this is important for mixing purposes - and induce significant shear and extensional stresses, which may promote important viscous dissipation. Figure 7.14 presents a series of sequential pictures describing the progress along two kneading blocks having different staggering geometries of a liquid tracer injected into a highly viscous Newtonian silicone oil ($1000\ Pa \cdot s$) [145, 146]. In the case of the kneading block with disks staggered at 90° (Figure 7.14a) there is hardly any flow accumulation upstream (although this also depends on the relative magnitude of output and screw speed) and the repetitive flow division and merging along the block is evident. When a more restrictive geometry is used (in this case, a kneading block staggered at -30°, followed by a left-handed element, Figure 7.14b), several screw turns upstream work fully filled. In due course, the material progresses downstream along the channels created by the staggered disks. In both situations, the rotation of the disks also subjects the flow to a kneading effect (hence their designation). Generally, when the material supplied to the extruder attains the first screw restrictive section it melts rapidly, due to the combined contribution of local frictional forces, repetitive material compression, and heat transfer [147, 148]. Melting in a twin-screw extruder is much more rapid than in a single screw machine, although a clear understanding of the underlying mechanisms is still lacking (see, for example, References [149-155]). In any case, melting is controlled by screw design, operational parameters, and thermophysical properties of the material.

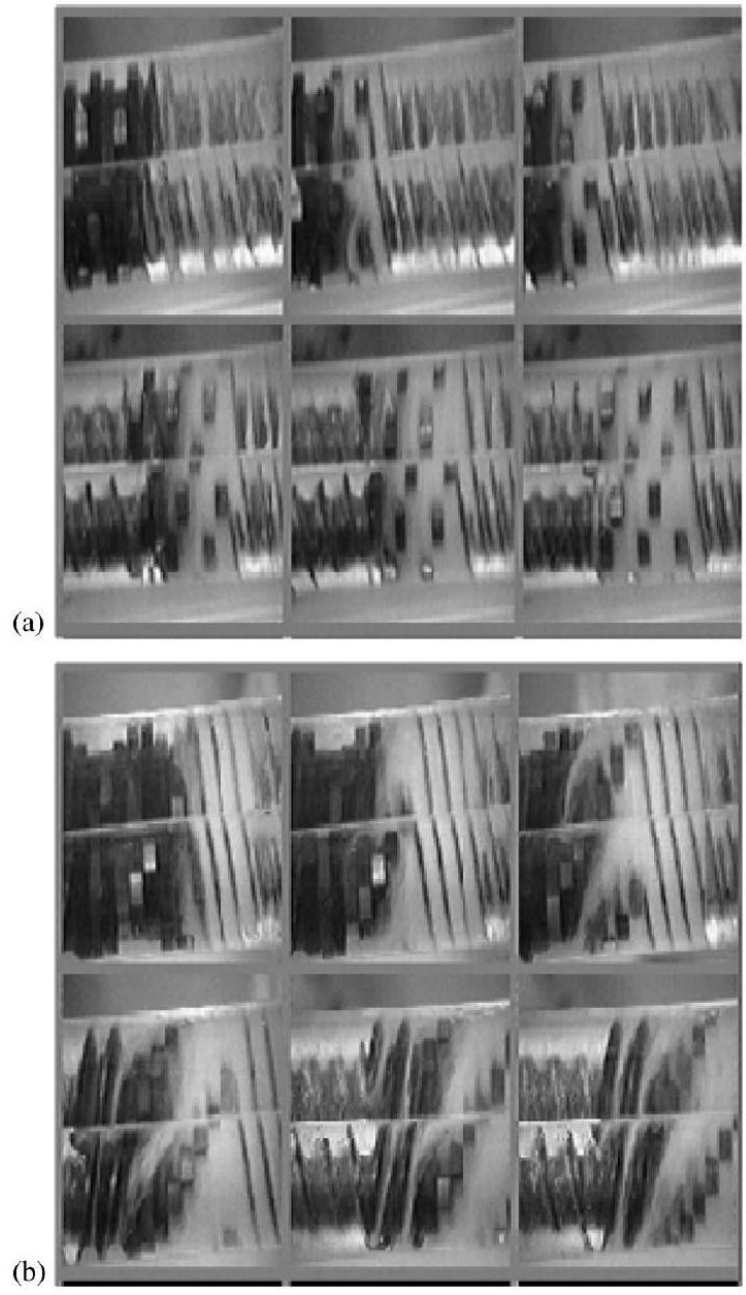

Figure 7.14 Flow visualization for a highly viscous silicone oil along the mixing zone of a twin-screw extruder: (a) orthogonal kneading block (90°); (b) kneading block with negative staggering $(-30^{\circ}C)$, plus left-handed element [146].

2

Evolution Along the Extruder

Generally, reactive extrusion deals with high melt-viscosity systems and diffusion-based reactions. Moreover, chemical reactions also frequently entail a

morphology development (e.g., reactive blending, dynamic vulcanization) that progresses along the screw at a rate that depends on local temperatures, residence time, stress levels, and
velocity fields - these being mostly determined by the screw geometry and operating conditions. Nonetheless, the reactions are also controlled by specific parameters. For example, monitoring the grafting of maleic anhydride (MA) onto polyolefins with different ethene/propene ratios along the extruder axis showed that the MA-graft content followed the same profile as the peroxide decomposition profile, with the chemical reactions occurring along the extruder until the peroxide was fully converted [156].

Mixing is always very important in reactive extrusion, as the machine should efficiently generate the necessary contact areas between the ingredients. For instance, reactive functionalized polymers can then form in situ block or graft copolymers at the interface of the blend components. Kneading blocks can be designed to generate the extensive melt deformation and reorientation that are mandatory for distributive mixing (as determined by the flow field complexity, average shear rate, and time), while dispersion is governed by the intensity and type of the stresses induced (a strong extensional component is particularly effective for dispersion). As for the morphology development, it is now generally accepted that in the case of polymer blends it involves the formation of sheets or ribbons of the minor component due to the magnitude of the local stresses, which subsequently become unstable and give rise to the formation of a two-dimensional network. When this becomes also unstable, particles or droplets are finally formed [157-160]. In reactive compatibilization, the graft or block copolymers formed at the interface induce a large reduction both in the interfacial tension and in the dispersed phase coalescence due to steric stabilization [161, 162].

In any case, the evolution of the morphology (with time or, equivalently, along the screw length) is far from gradual, sudden changes in particle size or in chemical conversion having been reported. This is especially true for fast reactive systems, where melting is also determinant, as reactions start to occur once this step is initiated. The rheological modification of PP via peroxide induced controlled degradation is a good, but not unique, example of a fast rate reaction. It was demonstrated [163] that PP degradation occurs by chain scission and depends on the level of stresses imposed by the screw elements, on temperature, and on the concentration of the hydrogen-abstracting agent. The reaction was found to be extremely rapid, that is, most of it took place in the first kneading block, upon melting, when the peroxide decomposed and abstracted one hydrogen from the PP chain, facilitating the β-scission mechanism. Similarly, during the dynamic vulcanization of PE/EPDM blends using a resol-$SnCl_2$ system, it was observed that crosslinking of the EPDM phase took place mostly in the first kneading zone, reaching a plateau thereafter [164]. As for PA-6/EPM-g-MA blends, it was reported that although the material remained mostly solid immediately upstream of the first screw restrictive zone, the unreacted MA content had already decreased to less than half of its original value. One L/D

(screw length to diameter ratio) later, a fully melted conventional polymer blend morphology was present, with relatively good distributive and dispersive mixing levels, a further important reduction in MA having been measured [133, 165]. This means that the rubber phase was dispersed from a millimeter to a micrometer scale within a few seconds/screw lengths.

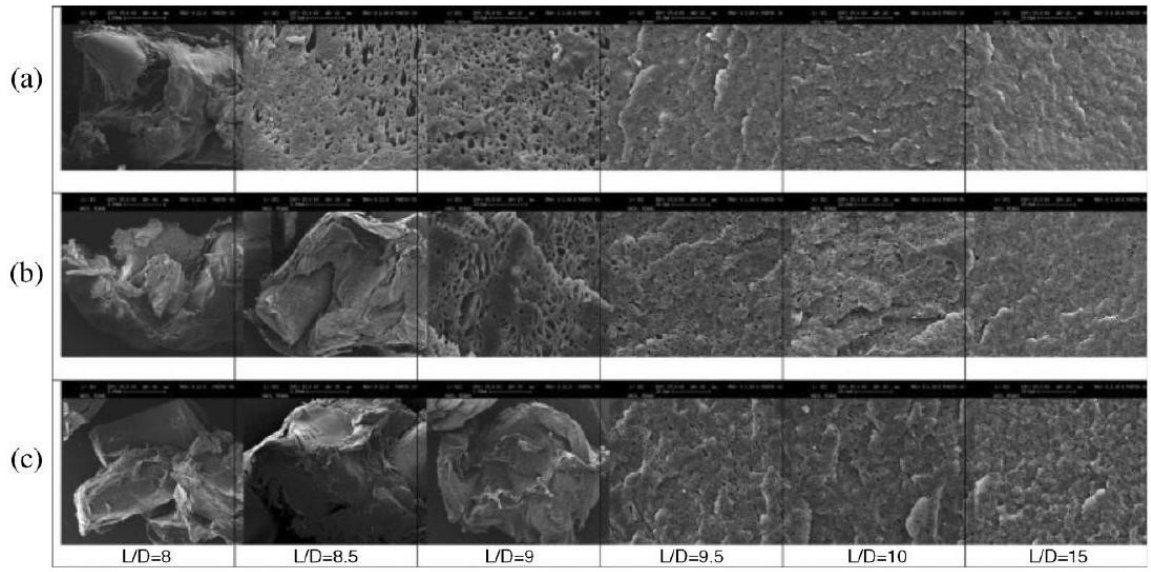

Figure 7.15 PA/PE blend morphology along the extruder for different screw speeds: 300 (a), 200 (b), and 100 rpm (c).

Recently [166], it has been suggested that melting (in terms of onset location and rate) may be the decisive parameter that influences chemical conversion and morphology evolution of fast reactive compatibilization systems. As seen in Figure 7.15 for a PA/PE system, melting in the co-rotating twin-screw extruder is very fast. In the three experiments, performed at different screw speeds, within 0.5 L/D there is a quick transition from a basically solid material to a more or less homogeneous melt. Although at 300 rpm a stable morphology seems to have been achieved around $L/D=9.5$, at 100 rpm this apparently happens only at $L/D=15$. As soon as one of the polymer components melts (in this case, PE), it surrounds, even if only partially, the other polymer pellets' surface. The interface thus generated allows straight away for high conversion ratios to be quickly attained. However, at this stage, this can only have a minor impact on the morphological development, as the magnitude of the material deformation does not generate new orders of magnitude of interfacial area, which in turn averts new major gains in chemical conversion. Thus, processing conditions inducing slow melting will also hold back chemical conversion. Considerable gains in interfacial area require full melting of the surviving solids. As this occurs, a dispersed phase is quickly created, and the formation of the copolymer (i.e., a further increase in chemical conversion) helps to swiftly stabilize the size and shape of the suspended particles, which evolve rapidly from large, elongated

particles to sub-micrometer regular units. This sequence of events is schematized in Figure 7.16, which illustrates also the effect of the screw speed.

3 Modeling and Optimization

Since reactive extrusion is an industrially relevant but complex technology, it seems important to develop theoretical approaches that can accurately predict the best conditions for carrying out successfully a practical reactive extrusion operation as well as to control the process. Two approaches have been adopted, one based on chemical engineering models, the other on continuum mechanics [137, 167]. The first considers the twin-screw extruder as a series of ideal chemical reactors (generally, continuous stirred-tank and/or plug-flow reactors) connected through direct flows and eventual leakage backflows. Mass balances for each reactor provide an approximation to the flow conditions. Similarly, energy balances and kinetic equations permit one to estimate the reactive process. Usually, these methods oversimplify the flow conditions and the parameters used need to be adjusted to each specific situation considered, which limits their predictive capacity and makes them useless for scaleup problems; however, because computations are quick, they can be useful for process control.

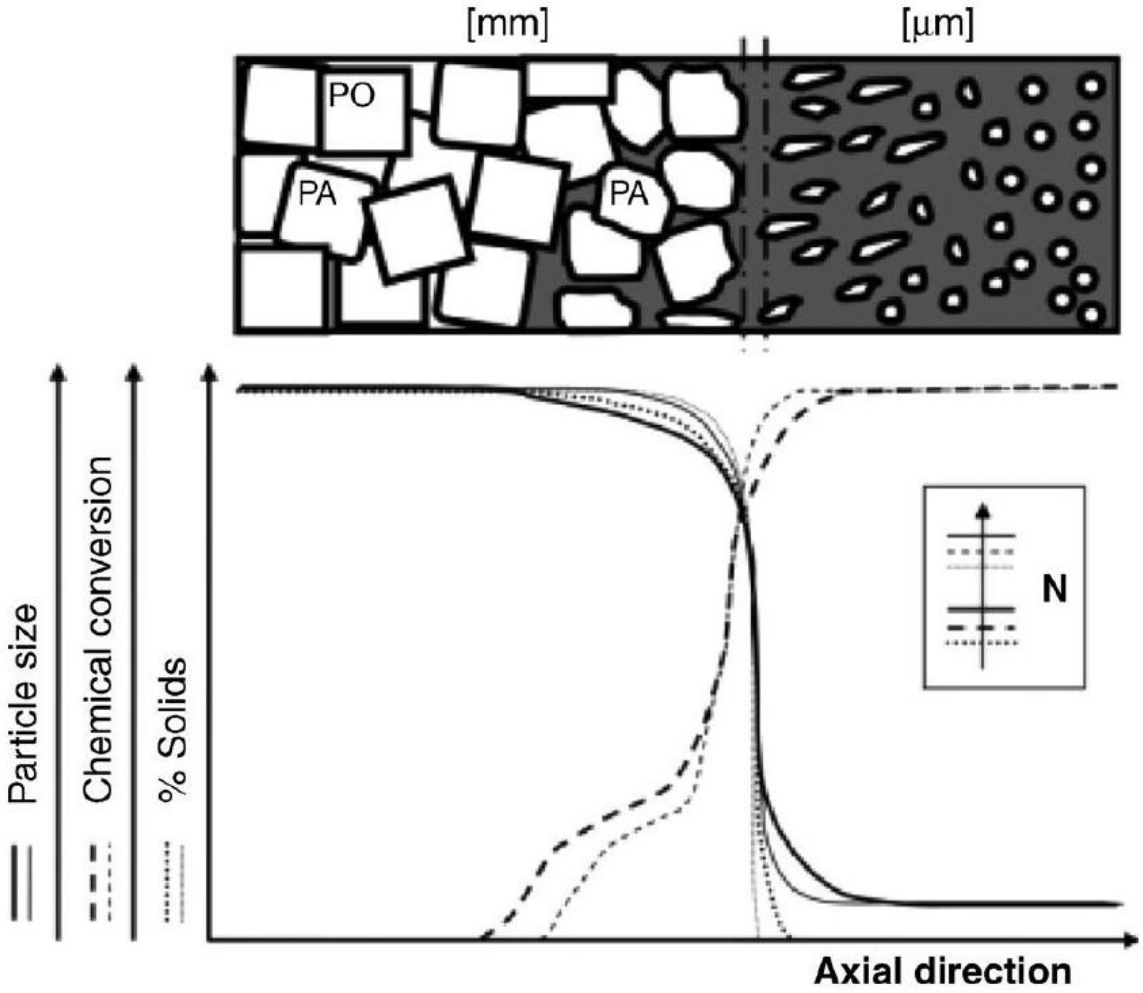

Figure 7.16 Schematic evolution of the physicochemical processes along the extruder during reactive polymer blending [166].

The second technique is based on continuum mechanics and requires three models that have to be inter-coupled:

1. The heat transfer and flow inside the extruder are calculated by solving the classical continuum mechanics equations (mass, momentum and energy balances), according to the local geometry and boundary conditions.
2. The rate of the chemical reaction can be expressed by a series of kinetic equations of the type:

$$\frac{-dc_j}{dt} = r(c_j, c_i, T) \qquad (7.2)$$

where c is concentration and subscript j refers to the reacting species in question and i to other reactants; the kinetic constants depend on local values of time, temperature, mixing conditions, concentration of reagents, and so on.

3) The variations of the physical and rheological properties of the material with the reaction are described by constitutive equations. In particular, changes in viscosity with reaction extent can encompass several orders of magnitude, so it is important to establish adequate rheokinetic relationships.

The reaction kinetics depend on the local values of temperature and residence time; in turn, their evolution changes the viscosity of the material, which affects the flow characteristics. To handle this interdependence, Vergnes and Berzin [167] developed a procedure that consists in performing an initial simulation of the flow in the extruder, to estimate the residence times, temperatures, and reaction extents. The local viscosity changes can then be calculated using the respective constitutive equation. Next, a second simulation is performed, coupling at each location the flow conditions, the reaction development, and the viscosity changes. This technique has predictive capacity but, because it is computationally demanding, cannot be used for control purposes. The two approaches have been adopted in the literature (see examples in References [14, 168, 169]).

Modeling the flow in twin-screw extruders is difficult because of the starve-fed conditions and of the intricacy of the channel geometry (that also changes significantly in the down-channel direction), which create a complex 3D strongly nonisothermal flow pattern. Generally, there are two types of programs (Cassagnau et al. [14] recently reviewed these efforts):

1. Global process analyses from hopper to die, which compute the average pressure, temperature, residence time, shear rate, shear stress, and degree of fill axial profiles for a given throughput and screw speed, together with total power consumption, or specific energy consumption. Often, these programs are based on simplified 1D or 2D flow descriptions. Several of them are available commercially [170], the underlying models and algorithms being also accessible in the literature (see, for example, References [171, 172]). As an example, Figure 7.17 illustrates the evolution of melt temperature and pressure along the axis of a twin-screw extruder, as predicted by the Ludovic [(1)] software. As shown in the figure and explained above, screw channels become fully filled upstream of, and during flow along, restrictive elements, simultaneously with the development of an important viscous dissipation. In a few programs, the calculations have been extended to reactive systems, yielding the reaction extent profile along the screw.
2. 3D flow simulations are applied for detailed local flow descriptions, producing accurate information on velocity, temperature, and stress fields, as well as flow trajectories, thus enabling one, for instance, to characterize local mixing conditions. Since the computational efforts involved are generally considerable, recent efforts resort to parallel computing and may be based on simplified fictitious domain methods coupled to a "level-set" approach to represent the rotating screws (e.g. in Reference [175], commercialized as XimeX [®] software).

Figure 7.18 depicts the particle distribution in a twin-screw element after a certain flow time, after having been initially inserted in the gap between the screws. A quantitative estimation of distributive mixing could be applied to this data.

Another theoretical approach worth mentioning is the attempt to develop tools that can optimize automatically the processing conditions and/or the screw geometry of a co-rotating twin-screw extruder. In the second case, the problem consists in selecting the most adequate location along the screw axis of an available number of screw elements, to maximize a process performance. Multi-objective evolutionary algorithms have been successfully used for this purpose and extension of the method to reactive extrusion has also been attempted [173].

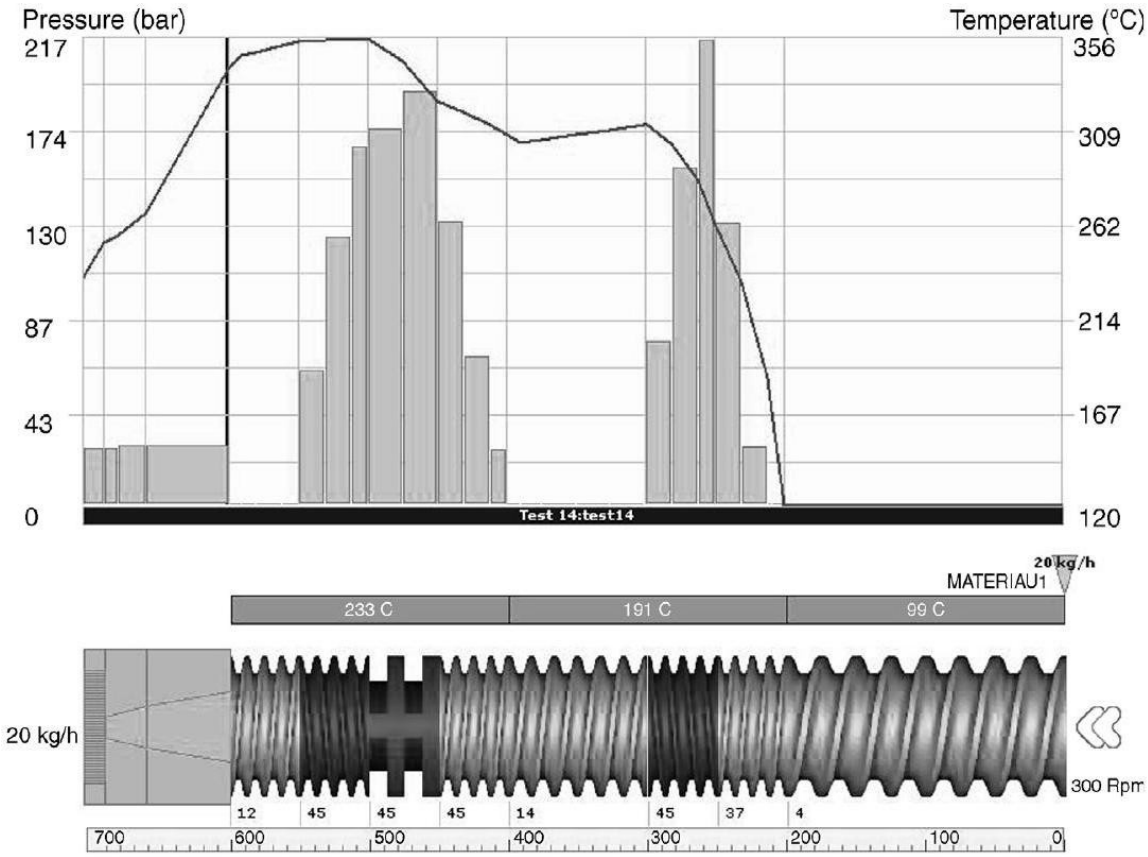

Figure 7.17 Temperature and pressure evolution along the screw profile, as predicted by Ludovic © V5.2 (http://www.scconsultants.com).

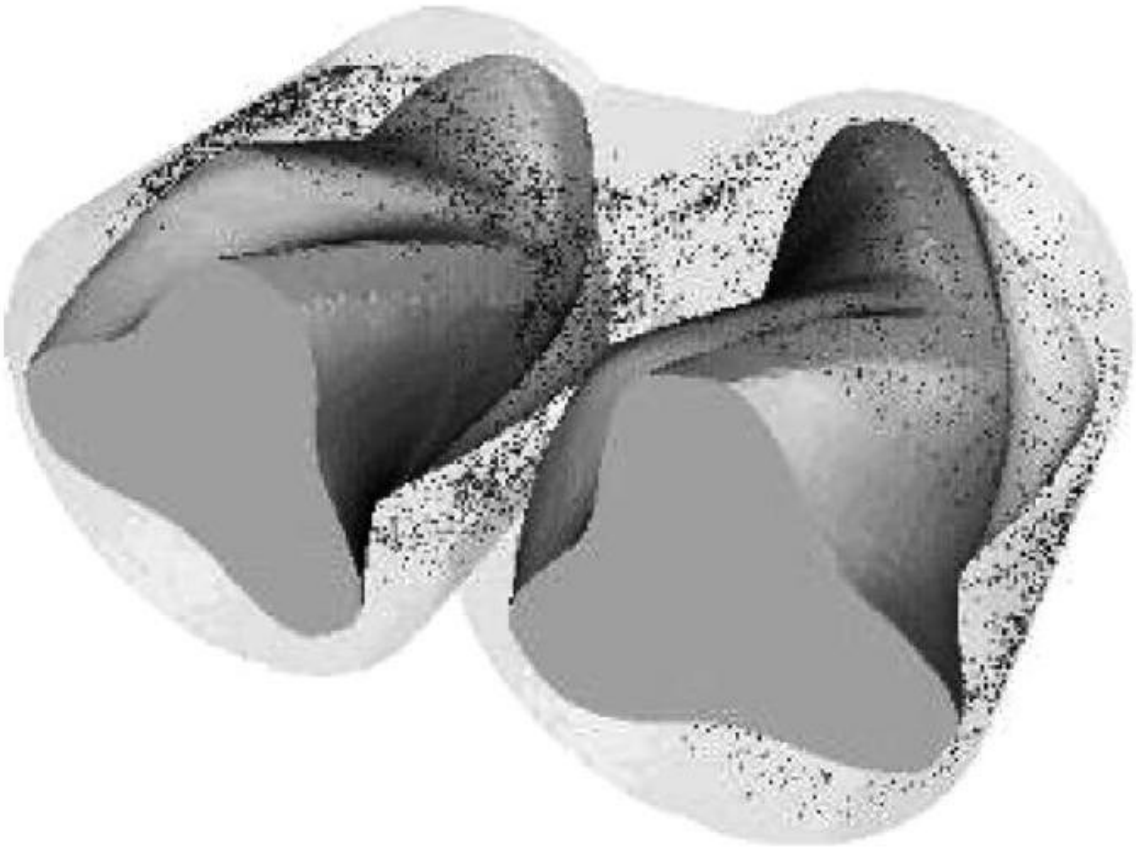

Figure 7.18 Particle distribution in a twin-screw element after a certain flow time, as predicted by Xime [8] (http://www.scconsultants.com).

A relevant example of optimization concerns the polymerization of ε-caprolactone, which was modeled by Poulesquen et al. [174]. Monomer [M_0] and activator $[I_0]$ are mixed at the entry of the extruder and polymerization (coordination-insertion mechanism) develops progressively. The objective is to reach full conversion at maximum output at the die exit, a major difficulty being the huge change in viscosity of the reactive system (from 10^{-3} to 10^{3} $Pa\ s$). Gaspar-Cunha et al. [173] applied an optimization algorithm to automatically establish the relative positions of ten screw elements (see dashed areas of the screws represented in Figure 7.19) that maximize output and minimize the melt temperature at the die exit (elements 1 and 2 on one end, and 13 and 14 on the opposite end, were kept unmoved during the optimization). Chemical conversion ratio was used as a restriction, that is, the solutions were taken as valid only if the conversion ratio at the screw end was higher than 99.9%. Since the reaction rate is controlled by the ratio between the initial monomer and initiator concentrations ([M_0]/$[I_0]$), independent runs were carried out using values of 400,800 , and 1000 . The optimal screw configurations that maximize output depend on the $[M_0]/[I_0]$ ratio. As this increases, the restrictive elements are located more downstream (and the set barrel temperature increases - not shown),

resulting in the efficient axial conversion profiles plotted in the figure.

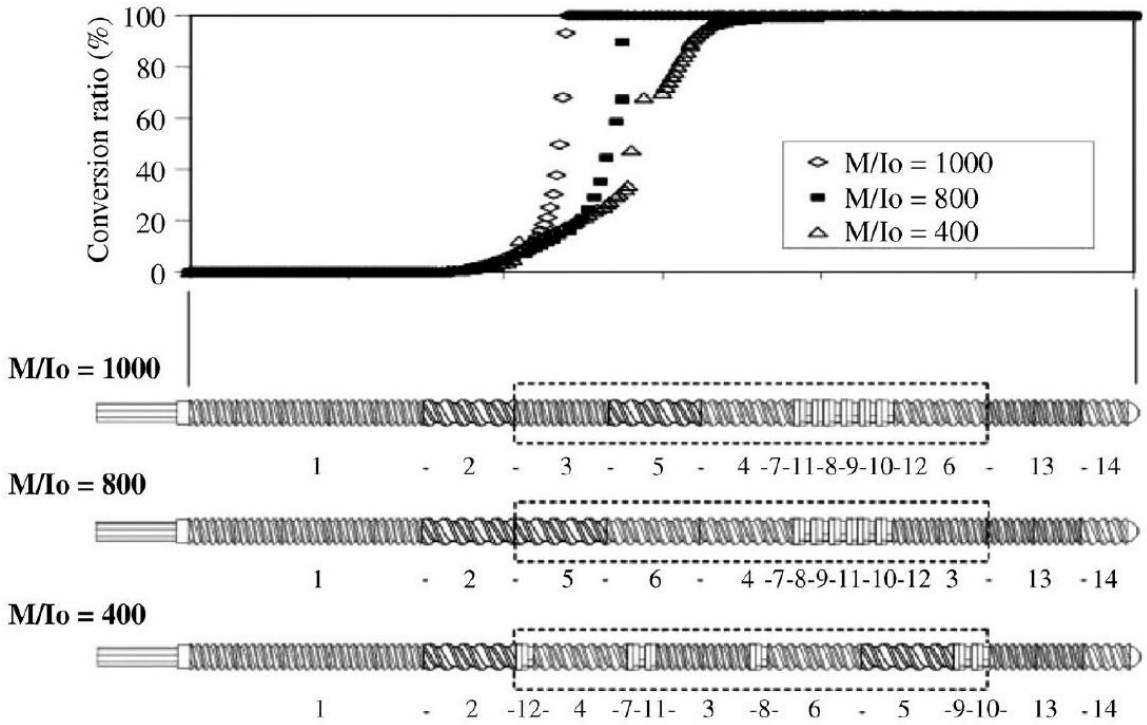

Figure 7.19 Best screw configurations for ε-caprolactone polymerization [173].

5 Conclusions

Throughout this chapter it was shown that compatibilization is a viable and costeffective way of controlling the morphology and morphology stability of immiscible polymer blends, thus converting these systems into successful materials for engineering applications.

The chapter concentrated on two major compatibilization routes, both using copolymers. In ex situ compatibilization, a pre-synthesized block or graft copolymer, whose segments are chemically identical to or have affinity with the blend components, are added to the system. The various types of copolymers, their molecular weight, and architecture can be used to control the final morphology. In the case of in situ compatibilization, the copolymer is formed at the interface, as a result of the reaction between the functional groups of the blend components. The location and functionality of the reactive groups, the precursors' molecular weight, and the flow characteristics determine the architecture of the copolymers produced as well as the interfacial characteristics. These were illustrated by examples of blends of PBT and PA-6.

Twin-screw extruders can be successfully used for industrial reactive blending. The evolution of chemical conversion and morphology development along the

screw of the high reactive systems that are usually converted in these machines is far from gradual. It was shown that melting is a major step for compatibilization, as significant interface regeneration and temperature rise are ensured. Modeling and optimization of reactive blending may contribute to a further increase of the present efficiency levels of this operation.

Abbreviations

Polymers and Monomers

ABS	Acrylonitrile, butadiene and styrene copolymer
AES	Acrylonitrile, ethylene and styrene copolymer
EA	Ethyl acrylate
EPM-g-MA	Ethylene and propylene monomer grafted with maleic anhydride
EPR	Ethylene and propylene rubber
GMA	Glycidyl methacrylate
HDPE	High density polyethylene
MGE	Methyl methacrylate, glycidyl methacrylate and ethyl acrylate copolymer
MMA	Methyl methacrylate
MMA-MA	Methyl methacrylate and maleic anhydride copolymer
PA-6	Polyamide 6
PA-6,6	Polyamide 6,6

PBT	Polybuthylene terephthalate
PC	Polycarbonate
PE	Polyethylene
PEO-b-PPO-b-PEO	Polyethylene oxide and polypropylene oxide copolymer
PET	Polyethylene terephthalate
PMMA	Polymethyl methacrylate
PP	Polypropylene

PP-g-MA	Polypropylene grafted with maleic anhydride
PS	Polystyrene
PS-b-PE	Polystyrene and polyethylene copolymer
PS-GMA	Polystyrene and glycidyl methacrylate copolymer
PS-g-PA-6	Polystyrene and polyamide 6 copolymer
PVP	Poly(2-vinylpyridine)
SAN	Styrene and acrylonitrile copolymer
SBS	Styrene, butadiene and styrene copolymer
SEBS	Styrene, ethylene, butylenes and styrene copolymer
SEBS-g-GMA	Styrene, ethylene, butylenes and styrene copolymer grafted with glycidyl methacrylate
SEBS-g-MA	Styrene, ethylene, butylenes and styrene copolymer grafted with maleic anhydride
SMA	Styrene maleic anhydride
sPS	Syndiotactic polystyrene

Others

Mc critical entanglement molecular weight
M_e molecular weight between entanglements
REX Reactive extrusion
SEM Scanning electron microscopy
TEM Transmission electron microscopy

References

1 Utracki, L.A. (1989) Polymer Alloys and Blends, Hanser Publishers, New York.
2 Paul, D.R., Barlow, J.W., and Keskkula, H. (1988) Polymer Blends, in Encyclopedia of Polymer Science and Engineering, vol. 12, 2nd edn (eds H.F. Mark, N.M. Bikales, C.G. Overberger, and G. Menges), WileyInterscience, New York, p. 399.
3 Paul, D.R. and Newman, S. (1979) Polymer Blends, Academic Press, New York.
4 Utracki, L.A. (1994) Encyclopaedic Dictionary of Commercial Polymer Blends, ChemTec Publishing, Toronto.

5 Datta, S. and Lohse, D. (1996) Polymeric Compatibilizers, Hanser Publishers, New York.
6 Koning, C., Duin, M., Pagnoulle, C., and Jerome, R. (1998) Prog. Polym. Sci.,

23, 707.
7 Gaylord, N. (1989) J. Macromol. Sci., 26, 1211.

8 Xanthos, M. and Dagli, S. (1991) Polym. Eng. Sci., 31, 929.
9 Triacca, V.J., Ziaee, S., Barlow, J.W., Keskkula, H., and Paul, D.R. (1991) Polymer, 32, 1401.

10 Dali, S.S., Xanthos, M., and Biesenberger, J.A. (1994) Polym. Eng. Sci., 43, 1720.
11 Machado, A.V., Yquel, V., Covas, J.A., Flat, J.-J., Ghamri, N., and Wollny, A. (2006) Macromol. Symp., 233, 86.

12 Xanthos, M. (1992) Reactive Extrusion: Principles and Practice, Hanser Publishers, New York.
13 Lambla, M. (1993) Reactive processing of thermoplastic polymers, in Comprehensive Polymer Science (eds G. Allen and J.C. Bewington), 1st supplement, Pergamon Press, New York.
14 Cassagnau, P., Bounor-Legare, V., and Fenouillot, F. (2007) Int. Polym. Proc., 3 (XXII), 218-258.
15 Leibler, L. (1982) Macromolecules, 15, 1283.

16 Noolandi, J. and Hong, M. (1982) Macromolecules, 15, 482.
17 Baker, W., Scott, C., and Hu, G.H. (2001) Reactive Polymer Blending, Hanser Publisher, Munich.
18 Ramic, A.J., Stehlin, J.C., Hudson, S.D., Jamieson, A.M., and Manas-Zloczower, I. (2000) Macromolecules, 33, 371-374.
19 Matos, M., Favis, B.D., and Lomellini, P. (1995) Polymer, 36, 3899.

20 Chio, W.M., Park, O.O., and Lim, J.G. (2004) J. Appl. Polym. Sci., 91, 3618.

21 Hong, B.K. and Jo, W.H. (2000) Polymer, 42, 1062.
22 Cigana, P., Favis, B.D., and Jerome, R. (1996) J. Polym. Sci. Part B, Polym. Phys., 34, 1691.
23 Cigana, P. and Favis, B.D. (1998) Polymer, 39, 3373.
24 Harrats, C., Fayt, R., and Jérôme, R. (2002) Polymer, 43, 863.

25 Zhang, C., Feng, L., Gu, X., Hoppe, S., and Hu, G.-H. (2007) Polymer, 48, 5940-5949.
26 Cimmino, S., Coppola, F., D'Orazio, L., Greco, R., Maglio, G., and Malinconico, M. (1986) Polymer, 27, 1874.

27 Chen, C. and White, J.L. (1993) Polym. Eng. Sci., 33, 923.
28 Carte, T.L. and Moet, A. (1993) J. Appl. Polym. Sci., 48, 611.

29 Kalfoglou, N.K., Skafidas, D.S., Kallitsis, J.K., Lambert, J.C., and Van der Stappen, L. (1995) Polymer, 36, 4453.
30 La Mantia, F.P., Vinci, M., and Pilati, F. (1994) Polym. Recycl., 1, 33.

31 Heino, M., Kirjava, J., Hietaoja, P., and Seppala, J. (1994) J. Appl. Polym. Sci., 54, 1613.
32 Creton, C., Kramer, E.J., and Hadziioannou, G. (1991) Macromolecules, 24, 1846.
33 Gallowaya, J., Jeon, H., Bellc, J., and Macosko, C. (2005) Polymer, 46, 183.

34 Willis, J.M. and Favis, B.D. (1988) Polym. Eng. Sci., 28, 1416.
35 Lee, J.D. and Yang, S.M. (1995) Polym. Eng. Sci., 35, 1821.
36 Fayt, R., Jerome, R., and Teyssie., Ph. (1989) J. Polym. Sci. Part B, Polym. Phys., 27, 775.
37 Hu, G.H., Sun, Y.J., and Lambla, M. (1996) Polym. Eng. Sci., 36, 676.

38 Sun, Y.J., Hu, G.H., Lambla, M., and Kotlar, H.K. (1996) Polymer, 25, 4119.

39 Anastasiadis, S., Gancarz, I., and Koberstein, J. (1989) Macromolecules, 22, 1449.

40 Hong, B.K. and Jo, W.H. (2000) Polymer, 41, 2069.
41 Macaúbas, P.H.P. and Demarquette, N.R. (2001) Polymer, 42, 2543.

42 Fredrickson, G.H. and Milner, S.T. (1996) Macromolecules, 29, 7386.
43 O'Shaughnessy, B. and Sawhney, U. (1996) Phys. Rev. Lett., 76, 3444.

44 O'Shaughnessy, B. and Sawhney, U. (1996) Macromolecules, 29, 7230.

45 O'Shaughnessy, B. and Vavylonis, D. (1999) Europhys. Lett., 45, 638.

46 O'Shaughnessy, B. and Vavylonis, D. (1999) Macromolecules, 32, 1785.

47 O'Shaughnessy, B. and Vavylonis, D. (2000) Phys. Rev. Lett., 84, 3193.

48 O'Shaughnessy, B. and Vavylonis, D. (2000) Eur. Phys. J. E, 1, 159.

49 Jeon, H.K. and Kim, J.K. (2000) Macromolecules, 33, 8200.
50 Guégan, P., Macosko, C.W., Ishizone, T., Hirao, A., and Nakahama, S. (1994) Macromolecules, 27, 4993.

51 Schulze, J.S., Cernohous, J.J., Hirao, A., Lodge, T.P., and Macosko, C.W. (2000) Macromolecules, 33, 1191.
52 Oyama, H.T. and Inoue, T. (2001) Macromolecules, 34, 3331.
53 Orr, C.A., Cernohous, J.J., Guegan, P., Hirao, A., Jeon, H.K., and Macosko, C.W. (2001) Polymer, 42, 8171.

54 Oyama, H.T., Ougizawa, T., Inoue, T., Weber, M., and Tamaru, K. (2001) Macromolecules, 34, 7017.
55 Yin, Z., Koulic, C., Pagnoulle, C., and Jérôme, R. (2003) Langmuir, 19, 453.
56 Jones, T.D., Schulze, J.S., Macosko, C.W., and Lodge, T.P. (2003) Macromolecules, 36, 7212.
57 Kim, H.Y., Jeong, U., and Kim, J.K. (2003) Macromolecules, 36, 1594.

58 Lyu, S., Cernohous, J.J., Bates, F.S., and Macosko, C.W. (1999) Macromolecules, 32, 106.

59 Kim, B.J., Kang, H., Char, K., Katsov, K., Fredrickson, G.H., and Kramer, E.J. (2005) Macromolecules, 38, 6106.

60 Zhang, J., Lodge, T.P., and Macosko, C.W. (2005) Macromolecules, 38, 6586.

61 Jiao, J., Kramer, E.J., de Vos, S., Möller, M., and Koning, C. (1999) Polymer, 40, 3585.
62 Jiao, J., Kramer, E.J., de Vos, S., Möller, M., and Koning, C. (1999) Macromolecules, 32, 6261.
63 Kim, J.K., Jeong, W., Son, J., and Jeon, H.K. (2000) Macromolecules, 33, 9161.
64 Shull, K.R. (1991) J. Chem. Phys., 94, 5723.

65 Yeung, C. and Herrmann, K.A. (2003) Macromolecules, 36, 229-237.
66 Jeon, H.K., Macosko, C.W., Moon, B., Hoye, T.R., and Yin, Z. (2004) Macromolecules, 37, 2563.
67 Zhao, W., Zhao, X., Rafailovich, M.H., Sololov, J., Compost, R.J., Smith, S.D., Satkowski, M., Russell, T.P., Dozier, W.D., and Mansfield, T. (1993) Macromolecules, 26, 561.
68 Jeon, H.K., Feist, B.J., Koh, S.B., Chang, K., Macosko, C.W., and Dion, R.P. (2004) Polymer, 45, 197.

69 Jeon, H.K., Hyun, T.O., and Kim, J.K. (2001) Polymer, 42, 3259.

70 Jeon, H.K. and Kim, J.K. (1998) Macromolecules, 31, 9273.
71 Yin, Z., Koulic, C., Pagnoulle, C., and Jérôme, R. (2001) Macromolecules, 34, 5132.

72 Yin, Z., Koulic, C., Jeon, H.K., Pagnoulle, C., Macosko, C.W., and Jérôme, R. (2002) Macromolecules, 35, 8917.
73 Helfand, E. and Tagami, Y. (1971) J. Polym. Sci., 9, 741.

74 Broseta, D., Fredrickson, G.H., Helfand, E., and Leibler, L. (1990) Macromolecules, 23, 132.
75 Moon, B., Hoye, T.R., and Macosko, C.W. (2002) Polymer, 43, 5501.

76 Kim, H.Y., Lee, D.H., and Kim, J.K. (2006) Polymer, 47, 5108.

77 Charoensirisomboon, P., Inoue, T., and Weber, M. (2000) Polymer, 41, 6907.
78 Charoensirisomboon, P., Chiba, T., Solomko, S.I., Inoue, T., and Weber, M. (1999) Polymer, 40, 6803.

79 Pan, L., Chiba, T., and Inoue, T. (2001) Polymer, 42, 8825.
80 Fetters, L.J., Lohse, D.L., Richter, D., Witten, T.A., and Zirkel, A. (1994) Macromolecules, 27, 4649.

81 Leibler, L. (1988) Makromol Chem. Macromol Symp, 16, 1.
82 Elemans, P.H.M. and Meijer, H.E.M. (1988) Polym. Eng. Sci., 28, 2751.

83 Karger-Kocsis, J. and Vergnes, B. (1996) Polym. Eng. Sci., 36, 1685.
84 Favis, B.D. and Chalifoux, J.P. (1988) Polymer, 29, 1761.
85 Scott, C.E. and Macosko, C.W. (1991) Polym. Bull., 26, 341.
86 Scott, C.E. and Macosko, C.W. (1994) Polymer, 35, 5422.
87 Sundararaj, U., Dori, Y., and Macosko, C.W. (1995) Polymer, 36, 1995.
88 Sundararaj, U. and Macosko, C.W. (1995) Macromolecules, 28, 2647.

89 Sundararaj, U. and. Macosko, C.W. (1996) Polym. Eng. Sci., 36, 1769.

90 Cartier, H. and Hu, G.H. (1999) J. Polym. Eng. Sci., 39, 996.
91 Duin, M., Gurp, M., Leemans, L., Walet, M., Aussems, M., Martin, P., Legras, R., Machado, A.V., and Covas, J.A. (2003) Macromol. Symp., 198, 135-145.

92 Machado, A.V., Covas, J.A., and van Duin, M. (1999) J. Appl. Polym. Sci., 71, 135-141.

93 Duin, M., Machado, A.V., and Covas, J.A. (2001) Macromol. Symp., 170, 29.

94 Minale, M., Mewis, J., and Moldenaers, P. (1998) AIChE J., 44, 943.

95 Lyu, S.P., Bates, F.S., and Macosko, C.W. (2002) AIChE J., 48, 7.

96 Milner, S.T. and Xi, H.W. (1996) J. Rheol., 40, 663.
97 Macosko, C.W., Guégan, P., Nakayama, A.K.K.A., Marechal, P., and Inoue, T. (1996) Macromolecules, 29, 5590.
98 Lyu, S., Jones, T.D., Bates, F.S., and Macosko, C.W. (2002) Macromolecules, 35, 7845.
99 Hage, E., Hale, W., Keskkula, H., and Paul, D.R. (1997) Polymer, 38, 3237.
100 Corte, L. and Leibler, L. (2007) Macromolecules, 40, 5606.
101 Borggreve, R.J.M., Gaymans, R.J., Schuijer, J., and Ingen Housz, J.F. (1987) Polymer, 28, 1489.
102 Wu, S.H. (1988) J. Appl. Polym. Sci., 35, 549. Proceeding 8th International Conference on Deformation, Yield and Fracture of Polymers, Churchill College, Cambridge, 8-11 April 1991, Plastic and Rubber Institute, London, 78.
103 Bartczak, Z., Argon, A.S., Cohen, R.E., and Weinberg, M. (1999) Polymer, 40, 2331.

104 Loyens, W. and Groenickx, G. (2002) Polymer, 43, 5679.
105 Wu, S. (1985) Polymer, 26, 1855.
106 Jiang, W., Liang, H., and Jiang, B. (1998) Polymer, 39, 4437.
107 Jiang, W., Liu, C., Wang, Z., An, L., Liang, H., Jiang, B., Wang, X., and Zhang, H. (1998) Polymer, 39, 3285.
108 Gan, P.P. and Paul, D.R. (1994) Polymer, 35, 3513.
109 Sun, Y.J., Hu, G.H., Lambla, M., and Kotlar, H.K. (1996) Polymer, 37, 4119.
110 Angew, H.M. (1992) Makromol. Chem., 196, 89.
111 Hale, W., Keskkula, H., and Paul, D.R. (1999) Polymer, 40, 3665.

112 Hale, W., Pessan, L.A., Keskkula, H., and Paul, D.R. (1999) Polymer, 40, 4237.
113 Ito, E.N., Pessan, L.A., Covas, J.A., and Hage, E. (2003) Int. Polym. Process., 18, 376.

114 Ambrósio, J.D., Larocca, N.M., Pessan, L.A., and Hage, E. (2010) Polym. Eng. Sci., 50, 2382.
115 Mantovani, G.L., Canto, L.B., Hage, E., and Pessan, L.A. (2001) Macromol. Symp., 176, 167.
116 Martin, P., Devaux, J., Legras, R., van Gurp, M., and van Duin, M. (2001) Polymer, 42, 2463.
117 Larocca, N.M., Hage, E. and Pessan, L.A. (2004) Polymer, 45, 5265.
118 Larocca, N.M., Hage, E., and Pessan, L.A. (2005) J. Polym. Sci. Part B: Polym. Phys., 43, 1244.
119 Canto, L.B., Torriani, I.L., Plivelic, T.S., Hage, E. and Pessan, L.A. (2007) Polym. Int., 56, 308.
120 Kitayama, N., Keskkula, H., and Paul, D.R. (2000) Polymer, 41, 8053.
121 Kudva, R.A., Keskkula, R.A., and Paul, D.R. (2000) Polymer, 41, 225.
122 Kudva, R.A., Keskkula, H., and Paul, D.R. (2000) Polymer, 41, 239.

123 Kudva, R.A., Keskkula, H., and Paul, D.R. (1998) Polymer, 39, 2447.

124 Araújo, E.M., Hage, E., and Carvalho, A.J.F. (2003) J. Appl. Polym. Sci., 87, 842.
125 Araújo, E.M., Hage, E., and Carvalho, A.J.F. (2003) J. Appl. Polym. Sci., 90, 3512.
126 Araújo, E.M., Hage, E., and Carvalho, A.J.F. (2003) J. Mater. Sci., 38, 3515.
127 Araújo, E.M., Hage, E., and Carvalho, A.J.F. (2003) J. Appl. Polym. Sci., 90, 2643.
128 Araújo, E.M., Hage, E., and Carvalho, A.J.F. (2004) J. Mater. Sci., 39, 1173.
129 Becker, D., Porcel, F., Hage, E., and Pessan, L.A. (2008) Polym. Bull., 61, 353.
130 Becker, D., Hage, E., and Pessan, L.A. (2010) J. Appl. Polym. Sci., 115, 2540.

131 Becker, D., Hage, E., and Pessan, L.A. (2007) J. Appl. Polym. Sci., 106, 3248.

132 Machado, A.V., Covas, J.A., and Duin, M. (2002) Polym. Eng. Sci., 42, 2032.

133 Machado, A.V., Covas, J.A., and Duin, M. (2001) J. Appl. Polym. Sci., 80, 1535.

134 Covas, J.A., Machado, A.V., and Duin, M. (2000) Adv. Polym. Technol., 19, 260.

135 Michaeli, W., Grefenstein, A., and Berghaus, U. (1995) Polym. Eng. Sci., 35, 1485.
136 Tzoganakis, C. (1989) Adv. Polym. Technol., 9, 321.
137 Sakai, T. (2008) Twin-screw extruders used for reactive design processing: design and application. Plastic Extrusion Asia 17-18 March 2008, Bangkok, Thailand.

138 Machado, A.V., Covas, J.A., Bounor-Legare, V., and Cassagnau, P. (2009) Reactive polymer processing and design of stable micro and nano structures, in Advances in Polymer Processing: Macro- to Nano-Scales (eds S. Thomas and Y. Weimin) Woodhead Publishing Ltd., UK, pp. 579-621.
139 Janseen, L.P.B.M. (1988) Polym. Eng. Sci., 38, 2010.
140 Isac, S.K. and George, K.E. (2001) J. Appl. Polym. Sci., 81, 2545.
141 Mack, W.A. and Herter, R. (1976) Chem., Eng. Progr., 72, 64.
142 Van Der Goot, A.J., Hettema, R., and Jansen, L.P.B.M. (1997) Polym. Eng. Sci., 37, 511.
143 Beyreuther, R., Tandler, B., Hoffmann, M., and Vogel, R. (2001) J. Mater. Sci., 36, 3103.

144 Martin, C. (2008) Twin screw extrusion - advances for compounding, devolatilization, and direct extrusion. Plastic Extrusion Asia 17-18 March 2008, Bangkok, Thailand.
145 Tang, H., Wrobel, L.C., and Fan, Z. (2003) Model. Simul. Mater. Sci. Eng., 11, 771.

146 Carneiro, O.S., Caldeira, G., and Covas, J.A. (1999) J. Mater. Process. Technol., 309, 92.
147 Gogos, C.C., Tadmor, Z., and Kim, M.H. (1998) Adv. Polym. Technol., 17, 285.
148 Zhu, L. and Narh, K.A. (2006) Simulation, 82, 543-548.
149 Bawiskar, S. and White, J.L. (1998) Polym. Eng. Sci., 38, 727-740.
150 Kim, D.S., Lee, B.K., Kim, H.S., Lee, J.W., and Gogos, C.G. (2001) Korea-Australia Rheol. J., 13, 89-95.

151 Vergnes, B., Souveton, G., Delacour, M.L., and Ainser, A. (2001) Int. Polym. Proc., 16, 351.
152 Liu, T., Wong, A.C.-Y., and Zhu, F. (2001) Int. Polym. Proc., 16, 113.
153 Yichong, G. and Fuhua, Z. (2003) Polym. Eng. Sci., 43, 306.
154 Chen, H., Sundararaj, U., Nandakumar, K., and Wetzel, M.D. (2004) Ind. Eng. Chem. Res., 43, 6822.
155 Garge, S.C., Wetzel, M.D., and Ogunnaike, B.A. (2007) Polym. Eng. Sci., 47, 1040.
156 Machado, A.V., Van Duin, M., and Covas, J.A. (2000) J. Polym. Sci. Part A: Polym. Chem., 38, 3919.
157 Sundararaj, U., Macosko, C.W., Rolando, R.J., and Chan, H.T. (1992) Polym. Eng. Sci., 32, 1814.
158 Scott, C.E. and Macosko, C.W. (1995) Polymer, 36, 461.
159 Majumdar, B., Paul, D.R., and Oshinski, A.J. (1997) Polymer, 38, 1787.
160 Lee, J.K. and Han, C.D. (2000) Polymer, 41, 1799.
161 Cho, K. and Li, F. (1991) Macromolecules, 24, 2752.
162 Creton, C., Hooker, J., and Shull, K.R. (2001) Langmuir, 17, 4948.

163 Machado, A.V., Maia, J.M., Canevarolo, S.V., and Covas, J.A. (2004) J. Appl. Polym. Sci., 91, 2711-2720.
164 Machado, A.V., van Duin, M., and Covas, J.A. (2006) Mater. Sci. Forum, 514-

516, 838.
165 Machado, A.V., Covas, J.A., and Duin, M. (1999) J. Polym. Sci. Part A: Polym. Chem., 37, 1311.
166 Yquel, V., Machado, A.V., Covas, J.A., and Flat, J.J. (2009) J. Appl. Polym. Sci., 114, 1768.

167 Vergnes, B. and Berzin, F. (2006) C.R. Chim., 9, 1409.
168 Jia, Y., Zhang, G., Wu, L., Sun, S., Zhao, G., and An, L. (2007) Polym. Eng. Sci, 47, 667-674.
169 Anon (2005) Plastics Additives Compound., March/April, 34.
170 Vergnes, B., Della Valle, G., and Delamare, L. (1998) Polym. Eng. Sci., 38, 121.

171 White, J.L., Keum, J., Jung, H.L., Ban, K., and Bumm, S. (2006) Polym. Plast. Technol. Eng., 45, 539.
172 Valette, R., Vergnes, B., and Coupez, T. (2008) Int. J. Mat. Form., 1, 1131.

173 Gaspar-Cunha, A., Covas, J.A., and Vergnes, B. (2005) Polym. Eng. Sci., 45, 1159.

174 Poulesquen, A., Vergnes, B., Cassagnau, P., Gimenez, J., and Michel, A. (2001) Int. Polym. Process., 16, 31.